Size-dependent behaviour of functionally graded sandwich microbeams based on the modified strain gradient theory

Armagan Karamanli[a], Thuc P. Vo[b,*]

[a]Faculty of Engineering and Natural Sciences, Mechatronics Engineering, Bahcesehir University, Istanbul, Turkey.

[b]School of Engineering and Mathematical Sciences, La Trobe University, Bundoora, VIC 3086, Australia

[*]Corresponding author. E-mail: armaganfatih.karamanli@eng.bau.edu.tr (A. Karamanli); t.vo@latrobe.edu.au (TP Vo)

Abstract

This paper studies the bending, buckling and free vibration analyses of functionally graded (FG) sandwich microbeams using the third-order beam theory. The modified strain gradient theory (MSGT) with three material length scale parameters (MLSPs) is used to capture the size effect. The Mori-Tanaka homogenization scheme is employed to model the material distributions through the thickness. Finite element model is formulated to solve the problems. Verification studies for epoxy and FG microbeams are carried out to validate of the present model. Comparisons of the results of three different models such as MSGT, the modified couple stress theory (MCST) and classical continuum theory (CCT) are presented. Effects of small size, gradient index, shear deformation and boundary conditions on the structural behaviours of microbeams are investigated. Some new results of FG sandwich microbeams for both models (MCST and MSGT) are presented for the first time and can be used as benchmark in future studies.

Keywords: Size effects, Modified strain gradient theory, FG sandwich microbeams, FEM

1. Introduction

One of the most important factors forcing the researchers/scientists to search and discover a new type of material for the engineering applications is the severity of the engineering problem to be solved to satisfy the requirements raised by the sectors such as aerospace, defense, nuclear energy, medical, automotive, etc. In 1984, Japanese scientists working on a space shuttle projects discovered a new type of material which is called as functionally graded material (FGM) to build a thermal barrier with high performance properties [1]. The material properties of FGM can be controlled smoothly and continuously in the desired directions with the inclusion of two or more different constitutes which can be usually metal and ceramic. As an advanced class of composite materials, FGMs enable to provide some additional roles due to their advantages over conventional laminated composites such as high modulus of elasticity to density ratio, high strength to density ratio, lightweight, free of internal boundaries and inter-laminar stress concentrations. Recent review study related to modelling, optimization and analysis of FG macro/micro/nano structures can be found [2].

The attractive features of the FGMs have been also used to meet the extreme demands associated with the design of the micro/nano electromechanical systems (MEMS/NEMS), atomic force microscopes and thin films [3-9]. It should be noted that the classical continuum theories (CCTs) cannot be used to investigate mechanical behaviour of the FGM small scale structures due to lacking a material length scale parameter (MLSP) which allows computing the size-dependent behaviour. The experiments show that to analyze the size-dependent behaviour of these FG structures, the employment of the higher-order continuum theories (HOCTs) with the MLSP is inevitable [10-12]. The researchers have been proposed many HOCTs to investigate structural responses of the small-scale structures [13-28]. It is noteworthy that there is still no alignment among the researchers regarding to the most acceptable HOCT in terms of accuracy, satisfying the boundary conditions, computational time, etc. for the analysis of micro/nano scale structures. A detailed review of the HOCTs can be found by the recent work by Thai et al. [29].

Among the HOCTs, the modified couple stress theory (MCST) proposed by Yang et al. [28] can be found the most effective one for the micro-scale structures due to consisting of only one MLSP which leads to have the symmetric couple stress tensor and makes the implementation of the theory simple with less computational time. On the other hand, the study given by Shu and Fleck [30] has shown that the MCST leads to underestimation of the size effect by neglecting the dilatation gradient and deviatoric stretch gradient tensors which are defined in the modified strain gradient theory (MSGT) [12]. The MSGT introduces three MLSPs related to the symmetric curvature, dilatation gradient and

deviatoric stretch gradient tensors which are associated with the higher order stress tensors in the constitutive equations. This theory has been successfully applied by many researchers for the isotropic structures [31-40], FG microshells/microplates [41-48] and only some of them are mentioned here. The natural frequencies of strain gradient FG cylindrical microshells are studied by Zhang et al. [41]. Sahmani and Ansari [42] study the vibration analysis of the FG strain gradient microplates by employing the Navier solution and a higher-order shear deformation theory. The first-order and third-order shear deformable strain gradient FG annular/circular plate models are presented based on the differential quadrature approach [43-44]. Thai et al. [45, 46] use the isogeometric analysis (IGA) to study the mechanical behaviour of the FG microplates for linear problem [45] and nonlinear bending under the static and dynamic loading conditions [46]. Thai et al. [47] and Farzam and Hassani [48] also used the IGA to present structural responses of FG sandwich strain gradient microplates. However, there are only few papers dealing with FG microbeams using the MSGT, especially for FG sandwich microbeams. Ansari et al. [49] present the natural frequencies of the FG Timoshenko microbeams. By using differential quadrature formulation, he and his colleagues later extend previous work [9] to the bending, elastic stability and natural frequency behaviours of FG Timoshenko microbeams and compare the results for three models [50] (MSGT, MCST and CCT). The generalized differential quadrature technique is also applied to perform nonlinear vibration analysis of the third-order shear deformable FG microbeams by Sahmani et al. [51]. By using a trigonometric beam theory, Akgoz and Civalek [52] and Lei et al. [53] present elastic stability analysis and flexural and free vibration analysis of the FG microbeams. Until now, only Thai et al. [54] investigated the size effect of the FG sandwich beams but using the MCST and Timoshenko theory. Based on the literature studies provided above, one can easily states that there is no study to investigate of the structural responses of FG sandwich microbeams based on the MSGT and the higher-order beam theory. This is complicated problems and needs further study.

This paper proposes a third-order beam theory (TOBT) incorporating strain gradient effects for the bending, free vibration and buckling responses of FG sandwich microbeams. The size effect is considered by the MSGT with three MLSPs while the material variations through the thickness is calculated by using the Mori-Tanaka homogenization scheme. Lagrange equations are used to construct the equations of motion. Verification studies for epoxy and FG microbeams are carried out to validate of the present model. Comparisons of the results of three different models including the MSGT, MCST and CCT are presented. Effects of small size, gradient index, shear deformation and

boundary conditions on the dimensionless fundamental frequencies (DFFs), critical buckling loads (DCBLs) and mid-span deflections (DMD) of microbeams are investigated.

2. Theory and Formulation

2.1 FG Sandwich Microbeam

Consider two types (Type A and Type B) of the FG sandwich microbeams with the length 'L' and height 'h' as illustrated in Fig. 1. Type A is made of ceramic core and FG skins while Type B consists of FG core and metal and ceramic skins. The material properties including Young modulus 'E', shear modulus 'G', Poisson's ratio 'ν' and mass density 'ρ' of the FG layers vary through the thickness. By using Mori-Tanaka homogenization scheme, the effective material properties including the Bulk modulus can be presented in the following form:

$$\frac{K(z)-K_2}{K_2-K_1}=\frac{V_1}{1+V_2\dfrac{K_1-K_2}{K_2+\dfrac{4}{3}G_2}} \tag{1a}$$

$$\frac{G(z)-G_2}{G_2-G_1}=\frac{V_1}{1+V_2\dfrac{G_1-G_2}{G_2+G_2\dfrac{9K_2+8G_2}{6K_2+12G_2}}} \tag{1b}$$

$$E(z)=\frac{9K(z)G(z)}{3K(z)+G(z)} \tag{1c}$$

$$\nu(z)=\frac{3K(z)-2G(z)}{6K(z)+2G(z)} \tag{1d}$$

$$\rho(z)=\rho_1V_1(z)+\rho_2V_2(z) \tag{1e}$$

where the indices 1 and 2 represent the ceramic and metal constitutes of the FG layers.

Figure 1 about here

The volume fractions of the ceramic phases for the Type A:

$$V_c{}^{(1)}(z)=\left(\frac{z-h_0}{h_1-h_0}\right)^{p_z} \quad for\ h_0\le z\ \le\ h_1 \tag{2a}$$

$$V_c{}^{(2)}(z)=1 \qquad for\ h_1\le z\ \le\ h_2 \tag{2b}$$

$$V_c{}^{(3)}(z)=\left(\frac{z-h_3}{h_2-h_3}\right)^{p_z} \quad for\ h_2\le z\ \le\ h_3 \tag{2c}$$

where p_z is the material gradient index. It is noteworthy that there is a relationship between the volume fractions of the metal and ceramic phases as $V_c(z) + V_m(z) = 1$.

The ceramic volume fractions for the Type B is defined as follows:

$$V_c^{(1)}(z) = 0 \qquad for\ h_0 \le z \le h_1 \tag{3a}$$

$$V_c^{(2)}(z) = \left(\frac{z - h_1}{h_2 - h_1}\right)^{p_z} \quad for\ h_1 \le z \le h_2 \tag{3b}$$

$$V_c^{(3)}(z) = 1 \qquad for\ h_2 \le z \le h_3 \tag{3c}$$

2.2 Modified Strain Gradient Theory (MSGT)

In the MSGT, strain energy for the linear elastic body can be expressed:

$$\mathcal{U} = \frac{1}{2}\int_V \left(\sigma_{ij}\varepsilon_{ij} + m_{ij}\chi_{ij} + p_i\gamma_i + \tau_{ijk}\eta_{ijk}\right)d\mathcal{V}, \quad i,j,k = 1,2,3 \tag{4}$$

where σ_{ij} is the stress tensor, ε_{ij} is the strain tensor, m_{ij} is the deviatoric part of the symmetric couple stress tensor and χ_{ij} is the symmetric curvature tensor, γ_i is the dilatation gradient tensor, η_{ijk} is the deviatoric stretch gradient tensor and p_i and τ_{ijk} are the higher order stress tensors associated with the dilatation gradient and deviatoric stretch gradient tensors.

The components of the strain, symmetric curvature, dilatation gradient and deviatoric stretch gradient tensors related to the components of the displacement vector (u_1, u_2, u_3) can be given in the form of:

$$\varepsilon_{ij} = \frac{1}{2}\left(\frac{\partial u_i}{\partial x_j} + \frac{\partial u_j}{\partial x_i}\right) \tag{5a}$$

$$\chi_{ij} = \frac{1}{4}\left(e_{imn}\frac{\partial^2 u_n}{\partial x_{mj}^2} + e_{jmn}\frac{\partial^2 u_n}{\partial x_{mi}^2}\right) \tag{5b}$$

$$\gamma_i = \frac{\partial \varepsilon_{mm}}{\partial x_i} \tag{5c}$$

$$\eta_{ijk} = \frac{1}{3}\left(\frac{\partial \varepsilon_{jk}}{\partial x_i} + \frac{\partial \varepsilon_{ki}}{\partial x_j} + \frac{\partial \varepsilon_{ij}}{\partial x_k}\right) - \frac{1}{15}\left[\delta_{ij}\left(\frac{\partial \varepsilon_{mm}}{\partial x_k} + 2\frac{\partial \varepsilon_{mk}}{\partial x_m}\right) + \delta_{jk}\left(\frac{\partial \varepsilon_{mm}}{\partial x_i} + 2\frac{\partial \varepsilon_{mi}}{\partial x_m}\right) + \delta_{ki}\left(\frac{\partial \varepsilon_{mm}}{\partial x_j} + 2\frac{\partial \varepsilon_{mj}}{\partial x_m}\right)\right] \quad (5d)$$

where e_{ijk} and δ_{ij} denote the permutation symbol and Kronecker delta, respectively.

The stress tensors; σ_{ij}, m_{ij}, p_i and τ_{ijk} can be presented by the following linear elastic constitutive relations:

$$\sigma_{ij} = \left(\frac{E(z)}{1+\nu(z)}\right)\varepsilon_{ij} + \left[\frac{\nu(z)E(z)}{(1+\nu(z))(1-2\nu(z))}\right]\varepsilon_{kk}\delta_{ij} \quad (6a)$$

$$p_i = \left(\frac{E(z){\ell_0}^2}{1+\nu(z)}\right)\gamma_i \quad (6b)$$

$$\tau_{ijk} = \left(\frac{E(z){\ell_1}^2}{1+\nu(z)}\right)\eta_{ijk} \quad (6c)$$

$$m_{ij} = \left(\frac{E(z){\ell_2}^2}{1+\nu(z)}\right)\chi_{ij} \quad (6d)$$

where ℓ_0, ℓ_1 and ℓ_2 are the material length scale parameter (MLSP) associated with the dilatation gradient, deviatoric stretch gradient and symmetric curvature. If one assigns $\ell_0 = \ell_1 = 0$, the modified couple stress theory (MCST) formulation is derived. Moreover, the classical continuum theory (CCT) can be obtained by setting $\ell_0 = \ell_1 = \ell_2 = 0$.

2.3 Third-order beam theory (TOBT) and Constitutive Equations

By using the TOBT, the displacement fields of the FG microbeams can be presented in the form of:

$$u_1(x,z,t) = U(x,z,t) = u(x,t) - f_1(z)\frac{\partial w_b(x,t)}{\partial x} + f_2(z)\frac{\partial w_s(x,t)}{\partial x} \quad (7a)$$

$$u_3(x,t) = W(x,t) = w_b(x,t) + w_s(x,t) \quad (7b)$$

$$f_1(z) = \frac{4z^3}{3h^2} \; and \; f_2(z) = z - \frac{8z^3}{3h^2} \quad (7c)$$

where $u, w_b \; and \; w_s$ are the axial displacement, bending component of the transverse displacement and shear component of the transverse displacement, respectively to be determined.

The only nonzero strains can be expressed:

$$\varepsilon_x = \frac{\partial U}{\partial x} = u' - f_1(z)w_b'' + f_2(z)w_s'' \tag{8a}$$

$$\varepsilon_{xz} = \frac{\gamma_{xz}}{2} = \frac{1}{2}\left(\frac{\partial W}{\partial x} + \frac{\partial U}{\partial z}\right) = \frac{1}{2}f_3(z)(\, w_b' + 2w_s') \tag{8b}$$

where $f_3(z) = 1 - 4z^2/h^2$.

The components of the symmetric curvature, dilatation gradient and deviatoric stretch gradient tensors can be written by using the Eq. (5) as follows:

$$\chi_{xy} = \frac{1}{4}[-(1 + f_1{}')w_b'' - (1 - f_2{}')w_s'' \,] \tag{9a}$$

$$\chi_{yz} = \frac{1}{4}(-f_1{}''w_b' + f_2{}''w_s') \tag{9b}$$

$$\gamma_x = u'' - f_1 w_b''' + f_2 w_s''' \tag{9c}$$

$$\gamma_z = -f_1{}'w_b'' + f_2{}'w_s'' \tag{9d}$$

$$\eta_{xxx} = \frac{1}{5}[2u'' - 2f_1 w_b''' - f_3{}'w_b' + 2f_2 w_s''' - 2f_3{}'w_s'] \tag{9e}$$

$$\eta_{zzz} = \frac{1}{5}[f_1{}'w_b'' - f_3 w_b'' - f_2{}'w_s'' - 2f_3 w_s''] \tag{9f}$$

$$\eta_{yyx} = \eta_{yxy} = \eta_{xyy} = \frac{1}{15}[-3u'' + 3f_1 w_b''' - f_3{}'w_b' - 3f_2 w_s''' - 2f_3{}'w_s'] \tag{9g}$$

$$\eta_{zzx} = \eta_{zxz} = \eta_{xzz} = \frac{1}{15}[-3u'' + 3f_1 w_b''' + 4f_3{}'w_b' - 3f_2 w_s''' + 8f_3{}'w_s'] \tag{9h}$$

$$\eta_{xxz} = \eta_{xzx} = \eta_{zxx} = \frac{1}{15}[-4f_1{}'w_b'' + 4f_3 w_b'' + 8f_3 w_s'' + 4f_2{}'w_s''] \tag{9i}$$

$$\eta_{yyz} = \eta_{yzy} = \eta_{zyy} = \frac{1}{15}[f_1{}'w_b'' - f_3 w_b'' - f_2{}'w_s'' - 2f_3 w_s''] \tag{9j}$$

$$\chi_{xx} = \chi_{yy} = \chi_{zz} = \chi_{xz} = \gamma_y = \eta_{zzy} = \eta_{zyz} = \eta_{yzz} = \eta_{yyy} = \eta_{xyz} = \eta_{yzx} = \eta_{zxy} = \eta_{xzy} = \eta_{zyx} = \eta_{yxz} = 0 \tag{9k}$$

The stress-strain relations for the FG microbeams can be expressed:

$$\begin{Bmatrix}\sigma_x\\ \sigma_{xz}\end{Bmatrix}=\begin{bmatrix}Q_{11} & 0\\ 0 & Q_{44}\end{bmatrix}\begin{Bmatrix}\varepsilon_x\\ \varepsilon_{xz}\end{Bmatrix} \tag{10a}$$

$$Q_{11}=E(z) \tag{10b}$$

$$Q_{44}=\frac{E(z)}{2(1+v(z))} \tag{10c}$$

$$\begin{Bmatrix}p_x\\ p_z\end{Bmatrix}=\frac{E(z){\ell_0}^2}{1+\nu(z)}\begin{Bmatrix}\gamma_x\\ \gamma_z\end{Bmatrix} \tag{10d}$$

$$\begin{Bmatrix}\tau_{xxx}\\ \tau_{zzz}\\ \tau_{xyy}\\ \tau_{xzz}\\ \tau_{zxx}\\ \tau_{zyy}\end{Bmatrix}=\frac{E(z){\ell_1}^2}{1+\nu(z)}\begin{Bmatrix}\eta_{xxx}\\ \eta_{zzz}\\ \eta_{xyy}\\ \eta_{xzz}\\ \eta_{zxx}\\ \eta_{zyy}\end{Bmatrix} \tag{10e}$$

$$\begin{Bmatrix}m_{xy}\\ m_{yz}\end{Bmatrix}=\frac{E(z){\ell_2}^2}{1+\nu(z)}\begin{Bmatrix}\chi_{xy}\\ \chi_{yz}\end{Bmatrix} \tag{10f}$$

2.4 Variational Formulation

By using the displacement field in Eq. (7), the strain energy of the FG microbeams can be expressed:

$$\mathcal{U}=\frac{1}{2}\int_V(\sigma_x\varepsilon_x+\sigma_{xz}\gamma_{xz}+p_x\gamma_x+p_z\gamma_z+\tau_{xxx}\eta_{xxx}+\tau_{zzz}\eta_{zzz}+3\tau_{xyy}\eta_{xyy}+3\tau_{xzz}\eta_{xzz}$$
$$+3\tau_{zxx}\eta_{zxx}+3\tau_{zyy}\eta_{zyy}+2m_{xy}\chi_{xy}+2m_{yz}\chi_{yz})dV \tag{11a}$$

$$\mathcal{U}=\frac{1}{2}\int_V\left[(Q_{11}{\varepsilon_x}^2+Q_{44}\varepsilon_{xz}\varepsilon_{xz})+\frac{E{\ell_0}^2}{1+\nu}({\gamma_x}^2+{\gamma_z}^2)+\frac{E{\ell_1}^2}{1+\nu}({\eta_{xxx}}^2+{\eta_{zzz}}^2+3{\eta_{xyy}}^2+3{\eta_{xzz}}^2\right.$$
$$\left.+3{\eta_{zxx}}^2+3{\eta_{zyy}}^2)+\frac{E{\ell_2}^2}{1+\nu}\left(2{\chi_{xy}}^2+2{\chi_{yz}}^2\right)\right]dV \tag{11b}$$

where

$${\varepsilon_x}^2=\left(\frac{\partial u}{\partial x}\right)^2+{f_1}^2\left(\frac{\partial^2 w_b}{\partial x^2}\right)^2+{f_2}^2\left(\frac{\partial^2 w_s}{\partial x^2}\right)^2-2f_1\left(\frac{\partial u}{\partial x}\right)\left(\frac{\partial^2 w_b}{\partial x^2}\right)+2f_2\left(\frac{\partial u}{\partial x}\right)\left(\frac{\partial^2 w_s}{\partial x^2}\right)$$
$$-2f_1f_2\left(\frac{\partial^2 w_b}{\partial x^2}\right)\left(\frac{\partial^2 w_s}{\partial x^2}\right) \tag{12a}$$

$$\gamma_{xz}{}^2 = (f_3)^2 \left[\left(\frac{\partial w_b}{\partial x}\right)^2 + 4\left(\frac{\partial w_s}{\partial x}\right)^2 + 4\left(\frac{\partial w_b}{\partial x}\right)\left(\frac{\partial w_s}{\partial x}\right) \right] \tag{12b}$$

$$2\chi_{xy}{}^2 = \frac{1}{8}\left[\left(1 + \frac{df_1}{dz}\right)^2 \left(\frac{d^2 w_b}{dx^2}\right)^2 + \left(1 - \frac{df_2}{dz}\right)^2 \left(\frac{d^2 w_s}{dx^2}\right)^2 + 2\left(1 + \frac{df_1}{dz}\right)\left(1 - \frac{df_2}{dz}\right)\left(\frac{d^2 w_b}{dx^2}\right)\left(\frac{d^2 w_s}{dx^2}\right) \right] \tag{12c}$$

$$2\chi_{yz}{}^2 = \frac{1}{8}\left[\left(\frac{d^2 f_1}{dz^2}\right)^2 \left(\frac{dw_b}{dx}\right)^2 + \left(\frac{d^2 f_2}{dz^2}\right)^2 \left(\frac{dw_s}{dx}\right)^2 - 2\left(\frac{d^2 f_1}{dz^2}\right)\left(\frac{d^2 f_2}{dz^2}\right)\left(\frac{dw_b}{dx}\right)\left(\frac{dw_s}{dx}\right) \right] \tag{12d}$$

$$\gamma_x{}^2 = \left(\frac{d^2 u}{dx^2}\right)^2 + f_1{}^2\left(\frac{d^3 w_b}{dx^3}\right)^2 + f_2{}^2\left(\frac{d^3 w_s}{dx^3}\right)^2 - 2f_1\left(\frac{d^2 u}{dx^2}\right)\left(\frac{d^3 w_b}{dx^3}\right) + 2f_2\left(\frac{d^2 u}{dx^2}\right)\left(\frac{d^3 w_s}{dx^3}\right) - 2f_1 f_2\left(\frac{d^3 w_b}{dx^3}\right)\left(\frac{d^3 w_s}{dx^3}\right) \tag{12e}$$

$$\gamma_z{}^2 = \left(\frac{df_1}{dz}\right)^2 \left(\frac{d^2 w_b}{dx^2}\right)^2 + \left(\frac{df_2}{dz}\right)^2 \left(\frac{d^2 w_s}{dx^2}\right)^2 - 2\left(\frac{df_1}{dz}\right)\left(\frac{df_2}{dz}\right)\left(\frac{d^2 w_b}{dx^2}\right)\left(\frac{d^2 w_s}{dx^2}\right) \tag{12f}$$

$$\eta_{xxx}{}^2 = \frac{1}{25}\left[4\left(\frac{d^2 u}{dx^2}\right)^2 - 8f_1\left(\frac{d^2 u}{dx^2}\right)\left(\frac{d^3 w_b}{dx^3}\right) - 4\left(\frac{df_3}{dz}\right)\left(\frac{d^2 u}{dx^2}\right)\left(\frac{dw_b}{dx}\right) + 8f_2\left(\frac{d^2 u}{dx^2}\right)\left(\frac{d^3 w_s}{dx^3}\right) - 8\left(\frac{df_3}{dz}\right)\left(\frac{d^2 u}{dx^2}\right)\left(\frac{dw_s}{dx}\right) + 4f_1{}^2\left(\frac{d^3 w_b}{dx^3}\right)^2 + \left(\frac{df_3}{dz}\right)^2\left(\frac{dw_b}{dx}\right)^2 + 4f_1\left(\frac{df_3}{dz}\right)\left(\frac{d^3 w_b}{dx^3}\right)\left(\frac{dw_b}{dx}\right) - 8f_1 f_2\left(\frac{d^3 w_b}{dx^3}\right)\left(\frac{d^3 w_s}{dx^3}\right) + 8f_1\left(\frac{df_3}{dz}\right)\left(\frac{d^3 w_b}{dx^3}\right)\left(\frac{dw_s}{dx}\right) - 4f_2\left(\frac{df_3}{dz}\right)\left(\frac{dw_b}{dx}\right)\left(\frac{d^3 w_s}{dx^3}\right) + 4\left(\frac{df_3}{dz}\right)^2\left(\frac{dw_b}{dx}\right)\left(\frac{dw_s}{dx}\right) + 4f_2{}^2\left(\frac{d^3 w_s}{dx^3}\right)^2 + 4\left(\frac{df_3}{dz}\right)^2\left(\frac{dw_s}{dx}\right)^2 - 8f_2\left(\frac{df_3}{dz}\right)\left(\frac{d^3 w_s}{dx^3}\right)\left(\frac{dw_s}{dx}\right) \right] \tag{12g}$$

$$\eta_{zzz}{}^2 = \frac{1}{25}\left[\left(\frac{df_1}{dz}\right)^2\left(\frac{d^2w_b}{dx^2}\right)^2 - 2\left(\frac{df_1}{dz}\right)f_3\left(\frac{d^2w_b}{dx^2}\right)^2 + (f_3)^2\left(\frac{d^2w_b}{dx^2}\right)^2\right.$$
$$- 2\left(\frac{df_1}{dz}\right)\left(\frac{df_2}{dz}\right)\left(\frac{d^2w_b}{dx^2}\right)\left(\frac{d^2w_s}{dx^2}\right) - 4\left(\frac{df_1}{dz}\right)(f_3)\left(\frac{d^2w_b}{dx^2}\right)\left(\frac{d^2w_s}{dx^2}\right)$$
$$+ 2\left(\frac{df_2}{dz}\right)(f_3)\left(\frac{d^2w_b}{dx^2}\right)\left(\frac{d^2w_s}{dx^2}\right) + 4(f_3)^2\left(\frac{d^2w_b}{dx^2}\right)\left(\frac{d^2w_s}{dx^2}\right) + \left(\frac{df_2}{dz}\right)^2\left(\frac{d^2w_s}{dx^2}\right)^2$$
$$\left. + 4\left(\frac{df_2}{dz}\right)(f_3)\left(\frac{d^2w_s}{dx^2}\right)^2 + 4(f_3)^2\left(\frac{d^2w_s}{dx^2}\right)^2\right] \qquad (12h)$$

$$3\eta_{xyy}{}^2 = \frac{3}{225}\left[9\left(\frac{d^2u}{dx^2}\right)^2 + 6\left(\frac{df_3}{dz}\right)\left(\frac{d^2u}{dx^2}\right)\left(\frac{dw_b}{dx}\right) - 18f_1\left(\frac{d^2u}{dx^2}\right)\left(\frac{d^3w_b}{dx^3}\right)\right.$$
$$+ 12\left(\frac{df_3}{dz}\right)\left(\frac{d^2u}{dx^2}\right)\left(\frac{dw_s}{dx}\right) + 18f_2\left(\frac{d^2u}{dx^2}\right)\left(\frac{d^3w_s}{dx^3}\right) + 9f_1{}^2\left(\frac{d^3w_b}{dx^3}\right)^2$$
$$- 6f_1\left(\frac{df_3}{dz}\right)\left(\frac{d^3w_b}{dx^3}\right)\left(\frac{dw_b}{dx}\right) + \left(\frac{df_3}{dz}\right)^2\left(\frac{dw_b}{dx}\right)^2 - 18f_1f_2\left(\frac{d^3w_b}{dx^3}\right)\left(\frac{d^3w_s}{dx^3}\right)$$
$$- 12f_1\left(\frac{df_3}{dz}\right)\left(\frac{d^3w_b}{dx^3}\right)\left(\frac{dw_s}{dx}\right) + 6f_2\left(\frac{df_3}{dz}\right)\left(\frac{dw_b}{dx}\right)\left(\frac{d^3w_s}{dx^3}\right)$$
$$+ 4\left(\frac{df_3}{dz}\right)^2\left(\frac{dw_b}{dx}\right)\left(\frac{dw_s}{dx}\right) + 9f_2{}^2\left(\frac{d^3w_s}{dx^3}\right)^2 + 4\left(\frac{df_3}{dz}\right)^2\left(\frac{dw_s}{dx}\right)^2$$
$$\left. + 12f_2\left(\frac{df_3}{dz}\right)\left(\frac{d^3w_s}{dx^3}\right)\frac{dw_s}{dx}\right] \qquad (12i)$$

$$3\eta_{xzz}{}^2 = \frac{3}{225}\Bigg[9\left(\frac{d^2u}{dx^2}\right)^2 - 18f_1\left(\frac{d^2u}{dx^2}\right)\left(\frac{d^3w_b}{dx^3}\right) - 24\left(\frac{df_3}{dz}\right)\left(\frac{d^2u}{dx^2}\right)\left(\frac{dw_b}{dx}\right)$$
$$+ 18f_2\left(\frac{d^2u}{dx^2}\right)\left(\frac{d^3w_s}{dx^3}\right) - 48\left(\frac{df_3}{dz}\right)\left(\frac{d^2u}{dx^2}\right)\left(\frac{dw_s}{dx}\right) + 9f_1{}^2\left(\frac{d^3w_b}{dx^3}\right)^2$$
$$+ 24f_1\left(\frac{df_3}{dz}\right)\left(\frac{d^3w_b}{dx^3}\right)\left(\frac{dw_b}{dx}\right) + 16\left(\frac{df_3}{dz}\right)^2\left(\frac{dw_b}{dx}\right)^2 - 18f_1f_2\left(\frac{d^3w_b}{dx^3}\right)\left(\frac{d^3w_s}{dx^3}\right)$$
$$+ 48f_1\left(\frac{df_3}{dz}\right)\left(\frac{d^3w_b}{dx^3}\right)\left(\frac{dw_s}{dx}\right) - 24f_2\left(\frac{df_3}{dz}\right)\left(\frac{dw_b}{dx}\right)\left(\frac{d^3w_s}{dx^3}\right)$$
$$+ 64\left(\frac{df_3}{dz}\right)^2\left(\frac{dw_b}{dx}\right)\left(\frac{dw_s}{dx}\right) + 9f_2{}^2\left(\frac{d^3w_s}{dx^3}\right)^2 - 48f_2\left(\frac{df_3}{dz}\right)\left(\frac{d^3w_s}{dx^3}\right)\left(\frac{dw_s}{dx}\right)$$
$$+ 64\left(\frac{df_3}{dz}\right)^2\left(\frac{dw_s}{dx}\right)^2\Bigg] \qquad (12j)$$

$$3\eta_{zxx}{}^2 = \frac{3}{225}\Bigg[16(f_3)^2\left(\frac{d^2w_b}{dx^2}\right)^2 - 32\left(\frac{df_1}{dz}\right)(f_3)\left(\frac{d^2w_b}{dx^2}\right)^2 + 16\left(\frac{df_1}{dz}\right)^2\left(\frac{d^2w_b}{dx^2}\right)^2$$
$$+ 64(f_3)^2\left(\frac{d^2w_b}{dx^2}\right)\left(\frac{d^2w_s}{dx^2}\right) - 64\left(\frac{df_1}{dz}\right)(f_3)\left(\frac{d^2w_b}{dx^2}\right)\left(\frac{d^2w_s}{dx^2}\right)$$
$$+ 32\left(\frac{df_2}{dz}\right)(f_3)\left(\frac{d^2w_b}{dx^2}\right)\left(\frac{d^2w_s}{dx^2}\right) - 32\left(\frac{df_1}{dz}\right)\left(\frac{df_2}{dz}\right)\left(\frac{d^2w_b}{dx^2}\right)\left(\frac{d^2w_s}{dx^2}\right)$$
$$+ 64(f_3)^2\left(\frac{d^2w_s}{dx^2}\right)^2 + 64\left(\frac{df_2}{dz}\right)f_3\left(\frac{d^2w_s}{dx^2}\right)^2 + 16\left(\frac{df_2}{dz}\right)^2\left(\frac{d^2w_s}{dx^2}\right)^2\Bigg] \qquad (12k)$$

$$3\eta_{zyy}{}^2 = \frac{3}{225}\Bigg[(f_3)^2\left(\frac{d^2w_b}{dx^2}\right)^2 - 2\left(\frac{df_1}{dz}\right)f_3\left(\frac{d^2w_b}{dx^2}\right)^2 + \left(\frac{df_1}{dz}\right)^2\left(\frac{d^2w_b}{dx^2}\right)^2$$
$$+ 4(f_3)^2\left(\frac{d^2w_b}{dx^2}\right)\left(\frac{d^2w_s}{dx^2}\right) - 4\left(\frac{df_1}{dz}\right)f_3\left(\frac{d^2w_b}{dx^2}\right)\left(\frac{d^2w_s}{dx^2}\right)$$
$$+ 2\left(\frac{df_2}{dz}\right)f_3\left(\frac{d^2w_b}{dx^2}\right)\left(\frac{d^2w_s}{dx^2}\right) - 2\left(\frac{df_1}{dz}\right)\left(\frac{df_2}{dz}\right)\left(\frac{d^2w_b}{dx^2}\right)\left(\frac{d^2w_s}{dx^2}\right) + 4(f_3)^2\left(\frac{d^2w_s}{dx^2}\right)^2$$
$$+ 4\left(\frac{df_2}{dz}\right)f_3\left(\frac{d^2w_s}{dx^2}\right)^2 + \left(\frac{df_2}{dz}\right)^2\left(\frac{d^2w_s}{dx^2}\right)^2\Bigg] \qquad (12l)$$

The potential energy of the axial N_0 and uniformly distributed q(x) loads is given by

$$V = -\frac{1}{2}\int_0^L N_0\left\{\left(\frac{\partial w_b}{\partial x}\right)^2 + 2\frac{\partial w_b}{\partial x}\frac{\partial w_s}{\partial x} + \left(\frac{\partial w_s}{\partial x}\right)^2\right\}dx - \int_0^L q(w_b + w_s)dx \tag{13}$$

The kinetic energy of the FG microbeams can be expressed:

$$K = \frac{1}{2}\int_0^L \left[I_0\left\{\left(\frac{\partial u}{\partial t}\right)^2 + \left(\frac{\partial w_b}{\partial t}\right)^2 + \left(\frac{\partial w_s}{\partial t}\right)^2 + 2\left(\frac{\partial w_b}{\partial t}\right)\left(\frac{\partial w_s}{\partial t}\right)\right\} - 2I_1\frac{\partial u}{\partial t}\frac{\partial^2 w_b}{\partial x \partial t} + I_2\left(\frac{\partial^2 w_b}{\partial x \partial t}\right)^2 + 2J_1\frac{\partial u}{\partial t}\frac{\partial^2 w_s}{\partial x \partial t} - 2J_3\frac{\partial^2 w_b}{\partial x \partial t}\frac{\partial^2 w_s}{\partial x \partial t} + K_1\left(\frac{\partial^2 w_s}{\partial x \partial t}\right)^2\right]dx \tag{14}$$

Here t is the time, and the inertial coefficients can be presented as

$$(I_0, I_1, I_2, J_1, J_3, K_1) = \int_{-\frac{h}{2}}^{+\frac{h}{2}} \rho\left(1, f_1, {f_1}^2, f_2, f_1 f_2, {f_2}^2\right)dz \tag{15}$$

2.5 Finite Element Formulation

FEM is developed here to solve the problems. The displacement functions $u(x,t)$, $w_b(x,t)$ and $w_s(x,t)$ can be expressed based on the two-node beam element and total energy by:

$$u(x,t) = \sum_{j=1}^{4} u_j \varphi_j(x) e^{i\omega t}, \tag{16a}$$

$$w_b(x,t) = \sum_{j=1}^{4} w_{b_j} \varphi_j(x) e^{i\omega t}, \tag{16b}$$

$$w_s(x,t) = \sum_{j=1}^{4} w_{s_j} \varphi_j(x) e^{i\omega t}, \tag{16c}$$

where ω is the natural frequency.

The unknows per element can be expressed in the form of:

$$u_j = \left[u^{(1)}, u_{,x}^{(1)}, u^{(2)}, u_{,x}^{(2)}\right] \tag{17a}$$

$$w_{b_j} = \left[{w_b}^{(1)}, {w_b}_{,x}^{(1)}, {w_b}^{(2)}, {w_b}_{,x}^{(2)}\right] \tag{17b}$$

$$w_{s_j} = \left[{w_s}^{(1)}, {w_s}_{,x}^{(1)}, {w_s}^{(2)}, {w_s}_{,x}^{(2)}\right] \tag{17c}$$

Hermite interpolation functions [30] for the displacement functions can be given as follows:

$$\varphi_1(x) = 1 - \frac{3x^2}{l^2} + \frac{2x^3}{l^3} \tag{18a}$$

$$\varphi_2(x) = x - \frac{2x^2}{l} + \frac{x^3}{l^2} \tag{18b}$$

$$\varphi_3(x) = \frac{3x^2}{l^2} - \frac{2x^3}{l^3} \tag{18c}$$

$$\varphi_4(x) = -\frac{x^2}{l} + \frac{x^3}{l^2} \tag{18d}$$

The total energy (Π) and equations of motion based on the Lagrange equations can be obtained in the following form:

$$\Pi = U + V - K \tag{19}$$

$$\frac{\partial \Pi}{\partial q_j} - \frac{d}{dt}\left(\frac{\partial \Pi}{\partial \dot{q}_j}\right) = 0 \tag{20}$$

where q_j representing the values of $(u_j, w_{b\,j}, w_{s\,j})$. The free vibration, stability and bending problems can be presented by using the following equations, respectively:

$$\left(\begin{bmatrix} [K_{11}] & [K_{12}] & [K_{13}] \\ [K_{12}]^T & [K_{22}] & [K_{23}] \\ [K_{13}]^T & [K_{23}]^T & [K_{33}] \end{bmatrix} - \omega^2 \begin{bmatrix} [M_{11}] & [K_{12}] & [K_{13}] \\ [M_{12}]^T & [M_{22}] & [M_{23}] \\ [M_{13}]^T & [M_{23}]^T & [M_{33}] \end{bmatrix}\right) \begin{Bmatrix} \{U\} \\ \{W_b\} \\ \{W_s\} \end{Bmatrix} = \begin{Bmatrix} \{0\} \\ \{0\} \\ \{0\} \end{Bmatrix} \tag{21a}$$

$$\left(\begin{bmatrix} [K_{11}] & [K_{12}] & [K_{13}] \\ [K_{12}]^T & [K_{22}] & [K_{23}] \\ [K_{13}]^T & [K_{23}]^T & [K_{33}] \end{bmatrix} - N_0 \begin{bmatrix} [0] & [0] & [0] \\ [0] & [G_{22}] & [G_{23}] \\ [0] & [G_{23}]^T & [G_{33}] \end{bmatrix}\right) \begin{Bmatrix} \{U\} \\ \{W_b\} \\ \{W_s\} \end{Bmatrix} = \begin{Bmatrix} \{0\} \\ \{0\} \\ \{0\} \end{Bmatrix} \tag{21b}$$

$$\begin{bmatrix} [K_{11}] & [K_{12}] & [K_{13}] \\ [K_{12}]^T & [K_{22}] & [K_{23}] \\ [K_{13}]^T & [K_{23}]^T & [K_{33}] \end{bmatrix} \begin{Bmatrix} \{U\} \\ \{W_b\} \\ \{W_s\} \end{Bmatrix} = \begin{Bmatrix} \{0\} \\ \{F_2\} \\ \{F_3\} \end{Bmatrix} \tag{21c}$$

where $[K_{kl}]$, $[M_{kl}]$ and $[G_{kl}]$ are the stiffness, mass and geometric stiffness matrices. F_k is the nodal force vector.

The components of the stiffness, mass and geometric stiffness matrices including the nodal force vectors are given by:

$$K_{11}(i,j) = \int_0^l A\,\varphi_{i,x}\varphi_{j,x}dx + \int_0^l \left[A_\gamma + \frac{2}{5}A_\eta\right]\varphi_{i,xx}\varphi_{j,xx}dx \qquad (22a)$$

$$K_{12}(i,j) = -\int_0^l B\,\varphi_{i,x}\varphi_{j,xx}dx - \int_0^l \left[B_\gamma + \frac{2}{5}B_\eta\right]\varphi_{i,xx}\varphi_{j,xxx}dx - \frac{1}{5}\int_0^l Y_\eta\,\varphi_{i,xx}\varphi_{j,x}dx \qquad (22b)$$

$$K_{13}(i,j) = \int_0^l B_s\,\varphi_{i,x}\varphi_{j,xx}dx + \int_0^l \left[C_\gamma + \frac{2}{5}C_\eta\right]\varphi_{i,xx}\varphi_{j,xxx}dx - \frac{2}{5}\int_0^l Y_\eta\,\varphi_{i,xx}\varphi_{j,x}dx \qquad (22c)$$

$$K_{22}(i,j) = \int_0^l \left[D + \frac{1}{8}A_\chi + H_\gamma + \frac{4}{15}Z_\eta + \frac{4}{15}S_\eta - \frac{8}{15}X_\eta\right]\varphi_{i,xx}\varphi_{j,xx}dx + \int_0^l \frac{1}{5}F_{s\eta}\,\varphi_{i,xxx}\varphi_{j,x}dx$$
$$+ \int_0^l \frac{1}{5}F_{s\eta}\,\varphi_{i,x}\varphi_{j,xxx}dx + \int_0^l \left[A_s + \frac{1}{8}P_\chi + \frac{4}{15}R_\eta\right]\varphi_{i,x}\varphi_{j,x}dx + \int_0^l \left[F_\gamma + \frac{2}{5}D_\eta\right]\varphi_{i,xxx}\varphi_{j,xxx}dx \qquad (22d)$$

$$K_{23}(i,j) = \int_0^l \left[-D_s + \frac{1}{8}B_\chi - Y_\gamma - \frac{4}{15}B_{s\eta} + \frac{4}{15}C_{s\eta} + \frac{8}{15}S_\eta - \frac{8}{15}X_\eta\right]\varphi_{i,xx}\varphi_{j,xx}dx$$
$$+ \int_0^l \left[2A_s - \frac{1}{8}R_\chi + \frac{8}{15}R_\eta\right]\varphi_{i,x}\varphi_{j,x}dx - \int_0^l \left[X_\gamma + \frac{2}{5}H_\eta\right]\varphi_{i,xxx}\varphi_{j,xxx}dx - \int_0^l \frac{1}{5}H_{s\eta}\,\varphi_{i,x}\varphi_{j,xxx}dx$$
$$+ \int_0^l \frac{2}{5}F_{s\eta}\,\varphi_{i,xxx}\varphi_{j,x}dx \qquad (22e)$$

$$K_{33}(i,j) = \int_0^l \left[H + \frac{1}{8}C_\chi + S_\gamma + \frac{4}{15}P_\eta + \frac{16}{15}C_{s\eta} + \frac{16}{15}S_\eta\right]\varphi_{i,xx}\varphi_{j,xx}dx - \frac{2}{5}\int_0^l H_{s\eta}\,\varphi_{i,xxx}\varphi_{j,x}dx$$
$$- \frac{2}{5}\int_0^l H_{s\eta}\,\varphi_{i,x}\varphi_{j,xxx}dx + \int_0^l \left[4A_s + \frac{1}{8}X_\chi + \frac{16}{15}R_\eta\right]\varphi_{i,x}\varphi_{j,x}dx$$
$$+ \int_0^l \left[R_\gamma + \frac{2}{5}F_\eta\right]\varphi_{i,xxx}\varphi_{j,xxx}dx \qquad (22f)$$

$$M_{11}(i,j) = \int_0^l I_0\, \varphi_i \varphi_j dx \qquad (22g)$$

$$M_{12}(i,j) = -\int_0^l I_1\, \varphi_i \varphi_{j,x} dx \qquad (22h)$$

$$M_{13}(i,j) = \int_0^l J_1\, \varphi_i \varphi_{j,x} dx \qquad (22i)$$

$$M_{22}(i,j) = \int_0^l I_0\, \varphi_i \varphi_j dx + \int_0^l I_2\, \varphi_{i,x} \varphi_{j,x} dx \qquad (22j)$$

$$M_{23}(i,j) = \int_0^l I_0\, \varphi_i \varphi_j dx - \int_0^l J_3\, \varphi_{i,x} \varphi_{j,x} dx \qquad (22k)$$

$$M_{33}(i,j) = \int_0^l I_0\, \varphi_i \varphi_j dx + \int_0^0 K_1\, \varphi_{i,x} \varphi_{j,x} dx \qquad (22l)$$

$$G_{22}(i,j) = -N_0 \int_0^l \varphi_{i,x} \varphi_{j,x}\, dx \qquad (22m)$$

$$G_{23}(i,j) = -N_0 \int_0^l \varphi_{i,x} \varphi_{j,x}\, dx \qquad (22n)$$

$$G_{33}(i,j) = -N_0 \int_0^l \varphi_{i,x} \varphi_{j,x}\, dx \qquad (22o)$$

$$F_2(i) = -\int_0^l q(x)\varphi_i \, dx \qquad (22p)$$

$$F_3(i) = -\int_0^l q(x)\varphi_i \, dx \qquad (22q)$$

The stiffness coefficients can be expressed by:

$$(A, B, B_s, D, D_s, H) = \int_{-h/2}^{+h/2} Q_{11}\left(1, f_1, f_2, {f_1}^2, f_1 f_2, {f_2}^2\right) dz \qquad (23a)$$

$$A_s = \int_{-h/2}^{+h/2} Q_{44} {f_3}^2 dz \qquad (23b)$$

$$(A_\chi, B_\chi, C_\chi, X_\chi, P_\chi, R_\chi)$$

$$= \int_{-h/2}^{+h/2} \frac{E{\ell_2}^2}{1+\nu}\left[(1+f_1')^2, (1+f_1')(1-f_2'), (1-f_2')^2, {f_2''}^2, {f_1''}^2, f_1'' f_2''\right] dz \qquad (23c)$$

$$(A_\gamma, B_\gamma, C_\gamma, F_\gamma, H_\gamma, X_\gamma, Y_\gamma, R_\gamma, S_\gamma) = \int_{-h/2}^{+h/2} \frac{E{\ell_0}^2}{1+\nu}\left[1, f_1, f_2, {f_1}^2, {f_1}'^2, f_1 f_2, f_1' f_2', {f_2}^2, {f_2}'^2\right] dz \quad (23d)$$

$$(A_\eta, B_\eta, C_\eta, D_\eta, F_\eta, H_\eta, X_\eta, Z_\eta, P_\eta, R_\eta, S_\eta, B_{s\eta}, C_{s\eta}, F_{s\eta}, H_{s\eta}, Y_{s\eta})$$

$$= \int_{-\frac{h}{2}}^{+\frac{h}{2}} \frac{E{\ell_1}^2}{1+\nu}\left[1, f_1, f_2, {f_1}^2, {f_2}^2, f_1 f_2, {f_1}' f_3, {f_1}'^2, {f_2}'^2, {f_3}'^2, {f_3}^2, \; {f_1}' {f_2}', {f_2}' f_3, f_1 {f_3}', f_2 {f_3}', {f_1}' {f_3}''\right] dz \quad (23e)$$

The kinematic boundary conditions (BCs) used for the numerical examples are given in Table 1.

Table 1 about here

3. Numerical Examples

In this section, several studies of FG sandwich microbeams on bending, vibration and buckling analysis are presented to validate the reliability of the present MSGT model. Unless stated otherwise, the Al/SiC microbeams (Al: $E_2 = E_m = 70\ GPa$, $\nu_2 = \nu_m = 0.3$, $\rho_m = 2702\ kg/m^3$; SiC: $E_1 = E_c = 427\ GPa$, $\nu_1 = \nu_c = 0.17$, $\rho_c = 3100\ kg/m^3$) are considered. These microbeams have various aspect ratios (L/h), dimensionless MLSP (h/ℓ) and boundary conditions (BCs). For the sake of simplicity, three MLSPs have the same value $\ell_0 = \ell_1 = \ell_2 = \ell$ and $\ell = 15\mu m$. The dimensionless fundamental frequency (DFF) (λ), dimensionless critical buckling load (DCBL) (N_{cr}) and dimensionless mid-span deflection (DMD) ($\overline{w}$) are defined in this paper, respectively:

$$\lambda = \frac{\omega L^2}{h}\sqrt{\frac{\rho_m}{E_m}} \tag{24a}$$

$$N_{cr} = N_0 \frac{12L^2}{E_c h^3} \tag{24b}$$

$$\overline{w} = w\frac{10^3 E_m h^3}{qL^4} \tag{24c}$$

3.1 Isotropic Epoxy Microbeams

The isotropic epoxy microbeams with the material properties: $E = 1.44\ GPa$, $\nu = 0.38$, $\rho = 1220\ kg/m^3$, $\ell = 17.6\ \mu m$ are considered. Convergence studies for a microbeam with ($L/h = 10$, $h/\ell = 2$) are carried out. The DFFs, DCBLs and DMDs are given in Table 2 and compared with the MSGT based on the Reddy beam theory (MSGT-RBT) [40]. Various uniform mesh distributions (30, 40, 50, 60, 70 and 80) are employed to compare the results with the previous ones. It is found that there is a good agreement between the numerical results and 70 uniformly distributed elements can produce satisfactory numerical results. Therefore, 70 uniformly distributed elements are used for the numerical examples in the following sections.

Table 2 about here

The calculated results in terms of DFF, DCBL and DMD for various (L/h), (h/ℓ) and BCs are given in Tables 3-6. They are compared with Navier and FEM solutions resulting from sinusoidal beam theory (MSGT-SBT [33]) and Reddy beam theory (MSGT-RBT [40]). It is observed that the current results are very close with those from previous ones thus the present theory is validated. As expected, the results from the MCST line between those from the MSGT and CCT. With the increase of (h/ℓ), the displacements increase and fundamental frequencies and critical buckling loads decrease. Due to decrement of beam's stiffness, the displacements obtained from MSGT are smaller as well as the natural frequencies and buckling loads are larger than those from the MCST.

Table 3 about here

Table 4 about here

Table 5 about here

Table 6 about here

3.2 FG Microbeams

For verification, Tables 7-9 show the DFFs, DCBLs and DMDs of the Al/SiC microbeams $(L/h = 10)$. It can be seen that the current results are in very good agreement with the referenced ones, which used the First-order beam theory (FBT [49]) and SBT [53]. By using the TOBT, the present results are closer with Lei et al. [53] and slight difference with Ansari et al. [49].

Table 7 about here

Table 8 about here

Table 9 about here

The ratios of the results obtained from the MSGT to those from the MCST of the microbeams with various BCs and $p_z = 5$ are plotted in Fig. 2. These ratios have the same trend regardless to BCs. Among them, the buckling ratio has the largest value and displacement ratio has the smallest one when $(h/\ell = 1)$. For example, these ratios are 0.332, 1.730 and 3.000 for displacement, frequency and buckling load of simply-supported beam with $p_z = 5$, respectively. It means that in this case when comparing with the MCST, displacement reduces 33% and buckling load increases 300%. This confirms that the MSGT with three MLSPs should be used to get better prediction for very small scales microbeams. When (h/ℓ) is relatively large $(h/\ell > 20)$ for vibration and buckling problems (Fig. 2a and b) or $(h/\ell > 40)$ for bending one (Fig. 2c), these ratios reach to unity. It implies that the components of dilatation and deviatoric stretch gradient become negligible and thus there is no different in results for two models (MSGT and MCST).

Figure 2 about here

Some new results for the DFFs, DCBLs and DMDs of the FG microbeams based on the MSGT and MCST models with $(h/\ell = 1, 2, 4\ and\ 8)$ and various material gradient indexes $(p_z = 0, 1, 2\ and\ 5)$ are given in Table 10.

Table 10 about here

Fig. 3 illustrates the DFFs, DCBLs and DMDs of the FG microbeams with respect to (h/ℓ) , p_z and (L/h). The deflections increase not only when p and (h/ℓ) increase but also when (L/h) decreases. The vibration mode shapes for cantilever beams are also plotted in Fig. 4.

Figure 3 about here

Figure 4 about here

3.2 FG Sandwich Microbeams

Type A and B with various schemes including (1-1-1), (1-2-1), (2-1-1) and (2-2-1) are considered. Since there is no results of these FG sandwich microbeams using the MSGT available, the present solutions are compared with those from the MCST based on the First-order beam theory (MCST-FBT [54]) in Tables 11-13. Some new results for both MCST and MSGT using the TOBT are also provided in Tables 14-16. Due to using the TOBT, the obtained results based on the MCST are slightly difference with the FBT solutions [54]. It can be observed from these tables that, for $p_z = 0$, all schemes for Type A give the same results but not for Type B. As expected, the DMDs obtained by the MSGT are lower than those of MCST, whereas the DFFs and DCBLs are bigger than corresponding ones.

Table 11 about here

Table 12 about here

Table 13 about here

Table 14 about here

Table 15 about here

Table 16 about here

Figs. 5 and 6 show the results of Type A and Type B with different schemes and (h/ℓ). The size effect on the bending behaviour is more considerable than that on the vibration and buckling one When (h/ℓ) is in the range [1-10] for vibration and buckling analysis or in the range [1-20] for bending one, the results change remarkably. When (h/ℓ) is outside these ranges and increases, they steadily become stable and finally converge to those from the CCT. Overall, the size effect can be neglected when $(h/\ell > 40)$ for all responses. Fig. 7 illustrates variation of frequencies for various schemes with respect to the size effect and power-law index.

Figure 5 about here

Figure 6 about here

Figure 7 about here

5. Conclusion

A size-dependent third-order beam model for FG sandwich microbeams is presented. The modified strain gradient theory with three material length scale parameters is used to capture the size effect. The governing equations are derived by using Lagrange equations and solved by FEM. Verification studies are carried out to validate of the present model. Effects of small size, gradient index, shear deformation and boundary conditions on the responses of microbeams are investigated. The size effects become significant for the FG sandwich microbeams when $(h/\ell < 10)$ for vibration and buckling problems and $(h/\ell < 20)$ for bending one. Some new results of FG sandwich microbeams for both models (MCST and MSGT) are presented for the first time and can be used as benchmark in future studies.

References

[1] Koizumi MFGM. FGM activities in Japan. Compos B Eng 1997;28(1–2):1–4.

[2] Ghatage P, Kar V, Sudhagar P. On the numerical modelling and analysis of multi-directional functionally graded composite structures: A review. Compos Struct. 2020;236:111837. doi:10.1016/j.compstruct.2019.111837

[3] Fu Y, Du H, Huang W, Zhang S, Hu M. TiNi-based thin films in MEMS applications: a review. Sensors and Actuators A: Physical. 2004;112(2-3):395-408. doi:10.1016/j.sna.2004.02.019

[4] Lee Z, Ophus C, Fischer L et al. Metallic NEMS components fabricated from nanocomposite Al–Mo films. Nanotechnology. 2006;17(12):3063-3070. doi:10.1088/0957-4484/17/12/042

[5] Baughman R. Carbon Nanotube Actuators. Science. 1999;284(5418):1340-1344. doi:10.1126/science.284.5418.1340

[6] Lau K, Cheung H, Lu J, Yin Y, Hui D, Li H. Carbon Nanotubes for Space and Bio-Engineering Applications. Journal of Computational and Theoretical Nanoscience. 2008;5(1):23-35. doi:10.1166/jctn.2008.003

[7] 2. Lü C, Lim C, Chen W. Size-dependent elastic behavior of FGM ultra-thin films based on generalized refined theory. Int J Solids Struct. 2009;46(5):1176-1185. doi:10.1016/j.ijsolstr.2008.10.012

[8] Rahaeifard M, Kahrobaiyan MH, Ahmadian MT. Sensitivity analysis of atomic force microscope cantilever made of functionally graded materials. ASME 2009 International Design Engineering Technical Conferences and Computers and Information in Engineering Conference 2009:539-544.

[9] Witvrouw A, Mehta A. The Use of Functionally Graded Poly-SiGe Layers for MEMS Applications. Materials Science Forum. 2005;492-493:255-260. doi:10.4028/www.scientific.net/msf.492-493.255

[10] Fleck N, Muller G, Ashby M, Hutchinson J. Strain gradient plasticity: Theory and experiment. Acta Metallurgica et Materialia. 1994;42(2):475-487. doi:10.1016/0956-7151(94)90502-9

[11] Stölken J, Evans A. A microbend test method for measuring the plasticity length scale. Acta Mater. 1998;46(14):5109-5115. doi:10.1016/s1359-6454(98)00153-0

[12] Lam D, Yang F, Chong A, Wang J, Tong P. Experiments and theory in strain gradient elasticity. J Mech Phys Solids. 2003;51(8):1477-1508. doi:10.1016/s0022-5096(03)00053-x

[13] Cosserat E, Cosserat F. Theory of deformable bodies. 1967;Washington, D.C.: National Aeronautics and Space Administration.

[14] Eringen A. Simple microfluids. Int J Eng Sci. 1964;2(2):205-217. doi:10.1016/0020-7225(64)90005-9

[15] Suhubi E, Eringen A. Nonlinear theory of micro-elastic solids—II. Int J Eng Sci. 1964;2(4):389-404. doi:10.1016/0020-7225(64)90017-5

[16] Eringen A. Micropolar fluids with stretch. Int J Eng Sci. 1969;7(1):115-127. doi:10.1016/0020-7225(69)90026-3

[17] Neff P, Forest S. A Geometrically Exact Micromorphic Model for Elastic Metallic Foams Accounting for Affine Microstructure. Modelling, Existence of Minimizers, Identification of Moduli and Computational Results. J Elast. 2007;87(2-3):239-276. doi:10.1007/s10659-007-9106-4

[18] Kröner E. Elasticity theory of materials with long range cohesive forces. Int J Solids Struct. 1967;3(5):731-742. doi:10.1016/0020-7683(67)90049-2

[19] Eringen A. Linear theory of nonlocal elasticity and dispersion of plane waves. Int J Eng Sci. 1972;10(5):425-435. doi:10.1016/0020-7225(72)90050-x

[20] Eringen A. Nonlocal polar elastic continua. Int J Eng Sci. 1972;10(1):1-16. doi:10.1016/0020-7225(72)90070-5

[21] Eringen A, Edelen D. On nonlocal elasticity. Int J Eng Sci. 1972;10(3):233-248. doi:10.1016/0020-7225(72)90039-0

[22] Mindlin R. Micro-structure in linear elasticity. Arch Ration Mech Anal. 1964;16(1):51-78. doi:10.1007/bf00248490

[23] Mindlin R. Second gradient of strain and surface-tension in linear elasticity. Int J Solids Struct. 1965;1(4):417-438. doi:10.1016/0020-7683(65)90006-5

[24] Toupin R. Elastic materials with couple-stresses. Arch Ration Mech Anal. 1962;11(1):385-414. doi:10.1007/bf00253945

[25] Toupin R. Theories of elasticity with couple-stress. Arch Ration Mech Anal. 1964;17(2):85-112. doi:10.1007/bf00253050

[26] Mindlin R, Tiersten H. Effects of couple-stresses in linear elasticity. Arch Ration Mech Anal. 1962;11(1):415-448. doi:10.1007/bf00253946

[27] Koiter WT. Couple stresses in the theory of elasticity. I and II Proc K Ned Akad Wet, 1964;B(67):17–44.

[28] Yang F, Chong A, Lam D, Tong P. Couple stress-based strain gradient theory for elasticity. Int J Solids Struct. 2002;39(10):2731-2743. doi:10.1016/s0020-7683(02)00152-x

[29] Thai H-T, Vo TP, Nguyen TK, Kim S. A review of continuum mechanics models for size-dependent analysis of beams and plates. Compos Struct. 2017;177:196-219. doi:10.1016/j.compstruct.2017.06.040

[30] Shu J, Fleck N. The prediction of a size effect in microindentation. Int J Solids Struct. 1998;35(13):1363-1383. doi:10.1016/s0020-7683(97)00112-1

[31] Kong S, Zhou S, Nie Z, Wang K. Static and dynamic analysis of micro beams based on strain gradient elasticity theory. Int J Eng Sci. 2009;47(4):487-498. doi:10.1016/j.ijengsci.2008.08.008

[32] Wang B, Zhao J, Zhou S. A micro scale Timoshenko beam model based on strain gradient elasticity theory. European Journal of Mechanics - A/Solids. 2010;29(4):591-599. doi:10.1016/j.euromechsol.2009.12.005

[33] Akgöz B, Civalek Ö. A size-dependent shear deformation beam model based on the strain gradient elasticity theory. Int J Eng Sci. 2013;70:1-14. doi:10.1016/j.ijengsci.2013.04.004

[34] Kahrobaiyan M, Asghari M, Ahmadian M. Strain gradient beam element. Finite Elements in Analysis and Design. 2013;68:63-75. doi:10.1016/j.finel.2012.12.006

[35] Wang B, Liu M, Zhao J, Zhou S. A size-dependent Reddy–Levinson beam model based on a strain gradient elasticity theory. Meccanica. 2014;49(6):1427-1441. doi:10.1007/s11012-014-9912-2

[36] Zhang B, He Y, Liu D, Gan Z, Shen L. Non-classical Timoshenko beam element based on the strain gradient elasticity theory. Finite Elements in Analysis and Design. 2014;79:22-39. doi:10.1016/j.finel.2013.10.004

[37] Wang B, Zhou S, Zhao J, Chen X. A size-dependent Kirchhoff micro-plate model based on strain gradient elasticity theory. European Journal of Mechanics - A/Solids. 2011;30(4):517-524. doi:10.1016/j.euromechsol.2011.04.001

[38] Ashoori Movassagh A, Mahmoodi M. A micro-scale modeling of Kirchhoff plate based on modified strain-gradient elasticity theory. European Journal of Mechanics - A/Solids. 2013;40:50-59. doi:10.1016/j.euromechsol.2012.12.008

[39] Wang B, Huang S, Zhao J, Zhou S. Reconsiderations on boundary conditions of Kirchhoff micro-plate model based on a strain gradient elasticity theory. Appl Math Model. 2016;40(15-16):7303-7317. doi:10.1016/j.apm.2016.03.014

[40] Zhang B, Li H, Kong L, Shen H, Zhang X. Size-dependent static and dynamic analysis of Reddy-type micro-beams by strain gradient differential quadrature finite element method. Thin-Walled Structures. 2019:106496. doi:10.1016/j.tws.2019.106496

[41] Zhang B, He Y, Liu D, Shen L, Lei J. Free vibration analysis of four-unknown shear deformable functionally graded cylindrical microshells based on the strain gradient elasticity theory. Compos Struct. 2015;119:578-597. doi:10.1016/j.compstruct.2014.09.032

[42] Sahmani S, Ansari R. On the free vibration response of functionally graded higher-order shear deformable microplates based on the strain gradient elasticity theory. Compos Struct. 2013;95:430-442. doi:10.1016/j.compstruct.2012.07.025

[43] Zhang B, He Y, Liu D, Lei J, Shen L, Wang L. A size-dependent third-order shear deformable plate model incorporating strain gradient effects for mechanical analysis of functionally graded circular/annular microplates. Composites Part B: Engineering. 2015;79:553-580. doi:10.1016/j.compositesb.2015.05.017

[44] Ansari R, Gholami R, Faghih Shojaei M, Mohammadi V, Sahmani S. Bending, buckling and free vibration analysis of size-dependent functionally graded circular/annular microplates based on

the modified strain gradient elasticity theory. European Journal of Mechanics - A/Solids. 2015;49:251-267. doi:10.1016/j.euromechsol.2014.07.014

[45] Thai S, Thai HT, Vo TP, Patel V. Size-dependant behaviour of functionally graded microplates based on the modified strain gradient elasticity theory and isogeometric analysis. Computers & Structures. 2017;190:219-241. doi:10.1016/j.compstruc.2017.05.014

[46] Thai S, Thai HT, Vo TP, Nguyen-Xuan H. Nonlinear static and transient isogeometric analysis of functionally graded microplates based on the modified strain gradient theory. Eng Struct. 2017;153:598-612. doi:10.1016/j.engstruct.2017.10.002

[47] Thai C, Ferreira A, Nguyen-Xuan H. Isogeometric analysis of size-dependent isotropic and sandwich functionally graded microplates based on modified strain gradient elasticity theory. Compos Struct. 2018;192:274-288. doi:10.1016/j.compstruct.2018.02.060

[48] Farzam A, Hassani B. Size-dependent analysis of FG microplates with temperature-dependent material properties using modified strain gradient theory and isogeometric approach. Composites Part B: Engineering. 2019;161:150-168. doi:10.1016/j.compositesb.2018.10.028

[49] Ansari R, Gholami R, Sahmani S. Free vibration analysis of size-dependent functionally graded microbeams based on the strain gradient Timoshenko beam theory. Compos Struct. 2011;94(1):221-228. doi:10.1016/j.compstruct.2011.06.024

[50] Ansari R, Gholami R, Faghih Shojaei M, Mohammadi V, Sahmani S. Size-dependent bending, buckling and free vibration of functionally graded Timoshenko microbeams based on the most general strain gradient theory. Compos Struct. 2013;100:385-397. doi:10.1016/j.compstruct.2012.12.048

[51] Sahmani S, Bahrami M, Ansari R. Nonlinear free vibration analysis of functionally graded third-order shear deformable microbeams based on the modified strain gradient elasticity theory. Compos Struct. 2014;110:219-230. doi:10.1016/j.compstruct.2013.12.004

[52] Akgöz B, Civalek Ö. A new trigonometric beam model for buckling of strain gradient microbeams. International Journal of Mechanical Sciences. 2014;81:88-94. doi:10.1016/j.ijmecsci.2014.02.013

[53] Lei J, He Y, Zhang B, Gan Z, Zeng P. Bending and vibration of functionally graded sinusoidal microbeams based on the strain gradient elasticity theory. International Journal of Engineering Science 2013;72(0):36 – 52.

[54] Thai HT, Vo TP, Nguyen TK, Lee J. Size-dependent behavior of functionally graded sandwich microbeams based on the modified couple stress theory. Compos Struct. 2015;123:337-349. doi:10.1016/j.compstruct.2014.11.065

Table 1. Kinematic boundary conditions used for the numerical computations.

BC	x=0	x=L
S-S	$u = 0, w_b = 0, w_s = 0$	$w_b = 0, w_s = 0$
C-C	$u = 0, w_b = 0, w_s = 0, {w_b}' = 0, {w_s}' = 0$	$u = 0, w_b = 0, w_s = 0, {w_b}' = 0, {w_s}' = 0$
C-S	$u = 0, w_b = 0, w_s = 0, {w_b}' = 0, {w_s}' = 0$	$w_b = 0, w_s = 0$
C-F	$u = 0, w_b = 0, w_s = 0, {w_b}' = 0, {w_s}' = 0$	

Table 2. Convergence studies for the epoxy microbeams ($\ell_0 = \ell_1 = \ell_2 = \ell = 17.6\mu m, L/h = 10, h/\ell = 2$)

Boundary conditions	Number of elements	Mid-span displacements	Fundamental frequencies	Critical buckling loads
S-S	30 elements	2.7777	4.6129	46.2268
	40 elements	2.7796	4.6121	46.1942
	50 elements	2.7806	4.6117	46.1774
	60 elements	2.7812	4.6115	46.1678
	70 elements	2.7816	4.6113	46.1618
	80 elements	2.7818	4.6112	46.1578
	Zhang et al. [40]	-	4.6029	45.4781
C-C	30 elements	0.6140	6.7671	169.2341
	40 elements	0.6156	6.7624	168.8160
	50 elements	0.6165	6.7600	168.6015
	60 elements	0.6170	6.7585	168.4782
	70 elements	0.6173	6.7577	168.4012
	80 elements	0.6175	6.7571	168.3499
	Zhang et al. [40]	-	6.8081	168.4851
C-S	30 elements	1.1573	5.7094	91.5563
	40 elements	1.1592	5.7071	91.4252
	50 elements	1.1602	5.7059	91.3580
	60 elements	1.1608	5.7052	91.3194
	70 elements	1.1611	5.7048	91.2952
	80 elements	1.1614	5.7045	91.2792
	Zhang et al. [40]	-	5.7051	90.0585
C-F	30 elements	9.3864	2.7684	11.8436
	40 elements	9.3917	2.7682	11.8414
	50 elements	9.3944	2.7681	11.8403
	60 elements	9.3960	2.7680	11.8397
	70 elements	9.3970	2.7679	11.8393
	80 elements	9.3977	2.7679	11.8390
	Zhang et al. [40]	-	2.7588	11.6309

Table 3. Comparison the mid-span deflections of the isotropic epoxy S-S microbeams under uniform load for various (L/h) and (h/ℓ) $(\ell_0 = \ell_1 = \ell_2 = \ell = 17.6\mu m)$

L/h	Theory	h/ℓ =1	5	10	∞
10	Present	0.7849	5.4766	6.7369	7.3005
	Zhang et al. [40] (MSGT-RBT)	0.7910	5.4894	6.7438	7.3005
	Akgoz and Civalek [33] (MSGT-SBT)	0.7742	5.4576	6.7317	7.2999
30	Present	0.7584	5.2621	6.4621	6.9940
	Zhang et al. [40] (MSGT-RBT)	0.7738	5.2920	6.4735	6.9940
	Akgoz and Civalek [33] (MSGT-SBT)	0.7576	5.2613	6.4619	6.9939
100	Present	0.7557	5.2389	6.4312	6.9591
	Zhang et al. [40] (MSGT-RBT)	0.7719	5.2696	6.4427	6.9591
	Akgoz and Civalek [33] (MSGT-SBT)	0.7557	5.2389	6.4312	6.9591

Table 4. Comparison the fundamental frequencies of the isotropic epoxy microbeams for various (L/h) and BCs ($\ell_0 = \ell_1 = \ell_2 = \ell = 17.6\mu m,\ h/\ell = 2$)

L/h	Theory	Boundary conditions (BCs)			
		S-S	C-C	C-S	C-F
5	Present	4.4864	6.3015	5.2419	2.7325
	Zhang et al. [40] (MSGT-RBT)	4.5070	6.4661	5.4957	2.7334
10	Present	4.6113	6.7577	5.7048	2.7679
	Zhang et al. [40] (MSGT-RBT)	4.6029	6.8081	5.7051	2.7588

Table 5. Comparison the critical buckling loads of the isotropic epoxy microbeams for various (L/h) and BCs $(\ell_0 = \ell_1 = \ell_2 = \ell = 17.6\mu m, h/\ell = 2)$

L/h	Theory	Boundary conditions (BCs)			
		S-S	C-C	C-S	C-F
5	Present	42.0581	129.4760	77.2679	11.5372
	Zhang et al. [40] (MSGT-RBT)	41.8017	135.5880	77.4234	11.3695
10	Present	46.1618	168.4012	91.2952	11.8393
	Zhang et al. [40] (MSGT-RBT)	45.4781	168.4851	90.0585	11.6309
100	Present	47.7621	190.8983	97.6832	11.9429
	Zhang et al. [40] (MSGT-RBT)	46.8664	187.2959	95.8423	11.7193

Table 6. Deflections, fundamental frequencies and critical buckling loads of the isotropic epoxy microbeams for various (L/h) and BCs $(\ell_0 = \ell_1 = \ell_2 = \ell = 17.6\mu m, h/\ell = 2)$

L/h	Theory		Boundary conditions			
			S-S	C-C	C-S	C-F
Mid-span deflections						
5	Present	CCT	14.3994	3.9202	6.5553	48.2829
		MCST	6.6457	1.5948	2.8712	22.3186
		MSGT	3.0461	0.8034	1.3831	10.0476
10	Present	CCT	13.3657	2.9406	5.5490	45.2887
		MCST	6.3417	1.3426	2.5943	21.5056
		MSGT	2.7796	0.6156	1.1592	9.3917
Critical buckling loads						
5	Present	CCT	8.9010	27.5381	16.5184	2.4020
		MCST	19.3076	65.6111	37.1397	5.0638
		MSGT	42.0581	129.4760	77.2679	11.5372
10	Present	CCT	9.6080	35.6040	19.1256	2.4507
		MCST	20.2553	77.2303	40.7351	5.1276
		MSGT	46.1618	168.4012	91.2952	11.8393
Fundamental frequencies						
5	Present	CCT	2.6701	5.1806	3.9282	0.9834
		MCST	3.9315	8.1375	5.9249	1.4346
		MSGT	5.8104	11.4628	7.9320	2.1554
10	Present	CCT	2.8002	6.0408	4.2975	1.0067
		MCST	4.0657	8.6455	6.2822	1.4579
		MSGT	6.1384	13.1826	9.3949	2.2117

Table 7. Comparison the deflections of Al/SiC S-S microbeams under uniform load for various (L/h), (h/l) and p_z $(\ell_0 = \ell_1 = \ell_2 = \ell = 15\mu m, L/h = 10)$

p_z	Theory		$h/\ell = 1$	2	4	8
0.3	Present	CCT	0.3394	0.3394	0.3394	0.3394
		MCST	0.0571	0.1518	0.2593	0.3150
		MSGT	0.0189	0.0646	0.1642	0.2678
	Lei et al. [53] (SBT)	CCT	0.3401	0.3401	0.3401	0.3401
		MCST	0.0571	0.1520	0.2597	0.3157
		MSGT	0.0186	0.0640	0.1635	0.2677
1	Present	CCT	0.4874	0.4874	0.4874	0.4874
		MCST	0.0868	0.2261	0.3781	0.4545
		MSGT	0.0287	0.0977	0.2439	0.3899
	Lei et al. [53] (SBT)	CCT	0.4872	0.4872	0.4872	0.4872
		MCST	0.0867	0.2260	0.3779	0.4543
		MSGT	0.0284	0.0967	0.2425	0.3890
4	Present	CCT	0.6356	0.6356	0.6356	0.6356
		MCST	0.1386	0.3341	0.5179	0.6014
		MSGT	0.0472	0.1546	0.3573	0.5318
	Lei et al. [53] (SBT)	CCT	0.6353	0.6353	0.6353	0.6353
		MCST	0.1385	0.3341	0.5179	0.6012
		MSGT	0.0467	0.1531	0.3552	0.5306

Table 8. Comparison the fundamental frequencies of Al/SiC S-S microbeams for various (h/l) $(\ell_0 = \ell_1 = \ell_2 = \ell = 15\mu m, L/h = 10, p_z = 2)$

Theory		$h/\ell = 1$	2	3	4	5
Present	CCT	0.3602	0.3602	0.3602	0.3602	0.3602
	MCST	0.8134	0.5131	0.4350	0.4040	0.3888
	MSGT	1.4027	0.7686	0.5786	0.4951	0.4512
Lei et al. [53] (SBT)	CCT	0.3607	0.3607	0.3607	0.3607	0.3607
	MCST	0.8150	0.5139	0.4356	0.4046	0.3894
	MSGT	1.4148	0.7734	0.5816	0.4972	0.4528
Ansari et al. [49] (FBT)	CCT	0.3617	0.3617	0.3617	0.3617	0.3617
	MCST	0.7983	0.5100	0.4341	0.4041	0.3894
	MSGT	1.2011	0.7346	0.5674	0.4903	0.4489

Table 9. Comparison the fundamental frequencies of Al/SiC S-S microbeams for various p_z ($\ell_0 = \ell_1 = \ell_2 = \ell = 15\mu m, L/h = 10, h/\ell = 2$)

Theory		$p_z = 0$	0.1	0.6	1.2	2	10
Present	CCT	0.5776	0.5137	0.4114	0.3771	0.3602	0.3235
	MCST	0.8592	0.7671	0.6116	0.5499	0.5131	0.4369
	MSGT	1.3134	1.1744	0.9356	0.8340	0.7686	0.6331
Lei et al. [53] (SBT)	CCT	0.5776	0.5129	0.4118	0.3776	0.3607	0.3237
	MCST	0.8592	0.7666	0.6123	0.5508	0.5139	0.4371
	MSGT	1.3210	1.1804	0.9412	0.8392	0.7734	0.6369
Ansari et al. [49] (FBT)	CCT	0.5776	0.5129	0.4121	0.3783	0.3617	0.3248
	MCST	0.8538	0.7619	0.6084	0.5470	0.5100	0.4332
	MSGT	1.2608	1.1276	0.8976	0.7986	0.7346	0.6033

Table 10. Dimensionless mid-span deflections, fundamental frequencies and critical buckling loads of Al/SiC microbeams for various (h/l) and p_z $(\ell_0 = \ell_1 = \ell_2 = \ell = 15\mu m, L/h = 10, h/\ell = 1, 2, 4, 8)$

BCs	h/ℓ	Mid-span deflections				Fundamental frequencies				Critical buckling loads			
		$p_z = 0$	1	2	5	$p_z = 0$	1	2	5	$p_z = 0$	1	2	5
S-S													
MCST	1	4.2228	10.7439	13.9195	18.5149	16.1144	10.4074	9.2461	8.1227	59.8509	23.5250	18.1584	13.6515
	2	11.3840	29.4831	37.2035	47.2598	9.8140	6.2851	5.6582	5.0856	22.1987	8.5718	6.7929	5.3472
	4	19.7637	52.2976	64.0210	77.4239	7.4479	4.7193	4.3135	3.9733	12.7850	4.8316	3.9466	3.2631
	8	24.2211	64.8486	78.1265	92.2027	6.7276	4.2380	3.9047	3.6409	10.4314	3.8961	3.2337	2.7396
MSGT	1	1.3887	3.4844	4.5462	6.1578	28.0963	18.2283	16.1333	14.0586	181.8811	72.5032	55.5759	41.0327
	2	4.7834	12.1274	15.6488	20.7358	15.1386	9.7970	8.7216	7.6760	52.8080	20.8321	16.1454	12.1848
	4	12.3380	31.9682	40.2007	50.8222	9.4260	6.0358	5.4432	4.9040	20.4755	7.9031	6.2846	4.9710
	8	20.4377	54.1508	66.1568	79.7628	7.3237	4.6378	4.2433	3.9145	12.3617	4.6657	3.8187	3.1669
C-F													
MCST	1	14.3350	36.4822	47.2714	62.8767	5.7687	3.7349	3.3186	2.9122	15.0808	5.9183	4.5656	3.4327
	2	38.6192	100.0430	126.2274	160.3000	3.5170	2.2572	2.0329	1.8263	5.6102	2.1636	1.7152	1.3519
	4	67.0090	177.3263	216.9901	262.2524	2.6724	1.6973	1.5527	1.4305	3.2425	1.2248	1.0023	0.8311
	8	82.1116	219.8313	264.7022	312.1607	2.4155	1.5254	1.4071	1.3126	2.6506	0.9900	0.8239	0.7008
MSGT	1	4.7520	11.7828	15.3884	20.8526	10.1303	6.5923	5.8306	5.0675	46.7322	18.5024	14.1318	10.4184
	2	16.1693	41.0311	52.9766	70.2088	5.4525	3.5321	3.1428	2.7627	13.5301	5.3105	4.1065	3.0977
	4	41.7566	108.2457	136.1151	172.0195	3.3898	2.1743	1.9614	1.7664	5.2251	2.0119	1.6001	1.2675
	8	69.2418	183.4726	224.0534	269.9484	2.6313	1.6700	1.5294	1.4113	3.1467	1.1869	0.9734	0.8099
C-C													
MCST	1	0.8760	2.2127	2.8593	3.8039	35.8303	23.2815	20.7159	18.1808	232.2130	91.8271	71.0311	53.3906
	2	2.3928	6.1616	7.7861	9.9439	21.6729	13.9490	12.5513	11.2417	85.1673	33.0440	26.1519	20.4902
	4	4.2248	11.1508	13.7565	16.8485	16.3057	10.3658	9.4392	8.6323	48.4005	18.3266	14.8701	12.1625
	8	5.2305	14.0025	17.0698	20.4897	14.6525	9.2488	8.4721	7.8259	39.2076	14.6420	12.0329	10.0514
MSGT	1	0.3095	0.7572	0.9747	1.3130	60.2190	39.7878	35.4785	30.9411	660.3701	269.4154	209.0688	155.1221
	2	1.0575	2.6292	3.3631	4.4488	32.5756	21.3470	19.0942	16.8043	193.3126	77.6240	60.6364	45.8287
	4	2.6969	6.9166	8.7001	11.0651	20.4003	13.1594	11.8686	10.6518	75.8760	29.5459	23.4884	18.4797
	8	4.4387	11.7246	14.4442	17.6524	15.9033	10.1066	9.2096	8.4312	46.1716	17.4678	14.1943	11.6359

Table 11. Dimensionless deflections of Al/SiC sandwich microbeams under uniform loads ($L/h = 10, h/l = 1\ and\ 5$)

h/ℓ	Types	Theory		Type A				Type B			
				$p_z = 0$	1	2	5	$p_z = 0$	1	2	5
1	1-1-1	Present	MCST	0.0352	0.0637	0.0722	0.0810	0.0523	0.0719	0.0763	0.0804
			MSGT	0.0116	0.0207	0.0235	0.0264	0.0167	0.0227	0.0241	0.0254
		Thai et. al. (FBT) [54]	MCST	0.0364	0.0648	0.0734	0.0824	0.0538	0.0752	0.0804	0.0856
	1-2-1	Present	MCST	0.0352	0.0541	0.0588	0.0633	0.0472	0.0755	0.0832	0.0907
			MSGT	0.0116	0.0176	0.0191	0.0206	0.0152	0.0240	0.0264	0.0289
		Thai et. al. (FBT) [54]	MCST	0.0364	0.0552	0.0598	0.0643	0.0485	0.0789	0.0878	0.0969
	2-1-1	Present	MCST	0.0352	0.0693	0.0805	0.0927	0.0652	0.0858	0.0903	0.0944
			MSGT	0.0116	0.0224	0.0261	0.0300	0.0205	0.0272	0.0287	0.0302
		Thai et. al. (FBT) [54]	MCST	0.0364	0.0707	0.0823	0.0953	0.0684	0.0912	0.0965	0.1016
	2-2-1	Present	MCST	0.0352	0.0594	0.0660	0.0726	0.0570	0.0866	0.0942	0.1018
			MSGT	0.0116	0.0192	0.0214	0.0235	0.0180	0.0276	0.0301	0.0328
		Thai et. al. (FBT) [54]	MCST	0.0364	0.0606	0.0673	0.0741	0.0589	0.0915	0.1003	0.1092
5	1-1-1	Present	MCST	0.1807	0.4700	0.5743	0.6763	0.3594	0.4727	0.4923	0.5067
			MSGT	0.1269	0.2832	0.3336	0.3833	0.2237	0.2999	0.3149	0.3274
		Thai et. al. (FBT) [54]	MCST	0.1811	0.4704	0.5750	0.6777	0.3606	0.4757	0.4968	0.5131
	1-2-1	Present	MCST	0.1807	0.3806	0.4430	0.5037	0.3078	0.4725	0.5036	0.5250
			MSGT	0.1269	0.2345	0.2642	0.2925	0.1961	0.3063	0.3309	0.3512
		Thai et. al. (FBT) [54]	MCST	0.1811	0.3809	0.4434	0.5041	0.3085	0.4751	0.5079	0.5318
	2-1-1	Present	MCST	0.1807	0.4997	0.6168	0.7255	0.4552	0.5157	0.5249	0.5320
			MSGT	0.1269	0.3043	0.3649	0.4247	0.2813	0.3398	0.3505	0.3597
		Thai et. al. (FBT) [54]	MCST	0.1811	0.5005	0.6184	0.7292	0.4592	0.5215	0.5317	0.5402
	2-2-1	Present	MCST	0.1807	0.4249	0.5072	0.5863	0.4004	0.5123	0.5299	0.5433
			MSGT	0.1269	0.2597	0.2997	0.3381	0.2466	0.3398	0.3586	0.3750
		Thai et. al. (FBT) [54]	MCST	0.1811	0.4253	0.5079	0.5876	0.4023	0.5166	0.5357	0.5508

Table 12. Dimensionless fundamental frequency of Al/SiC sandwich microbeams ($L/h = 10, h/l = 1\ and\ 5$)

h/ℓ	Types	Theory		Type A				Type B			
				$p_z = 0$	1	2	5	$p_z = 0$	1	2	5
1	1-1-1	Present	MCST	16.1144	12.2398	11.5846	11.0242	13.4761	11.5860	11.2813	11.0254
			MSGT	28.0963	21.4521	20.2842	19.2846	23.8255	20.5318	19.9821	19.5101
		Thai et. al. (FBT) [54]	MCST	15.8337	12.1351	11.4924	10.9287	13.3095	11.3842	11.0444	10.7472
	1-2-1	Present	MCST	16.1144	13.2122	12.7466	12.3567	14.1258	11.3043	10.8260	10.4192
			MSGT	28.0963	23.1699	22.3451	21.6475	24.8883	19.9873	19.1179	18.3544
		Thai et. al. (FBT) [54]	MCST	15.8337	13.0839	12.6357	12.2570	13.9514	11.1113	10.5946	10.1416
	2-1-1	Present	MCST	16.1144	11.7676	11.0072	10.3485	12.1704	10.6835	10.4442	10.2409
			MSGT	28.0963	20.6644	19.3390	18.1889	21.6050	18.8600	18.4035	18.0107
		Thai et. al. (FBT) [54]	MCST	15.8337	11.6506	10.8903	10.2074	11.9338	10.4206	10.1596	9.9337
	2-2-1	Present	MCST	16.1144	12.6499	12.0761	11.5914	12.9565	10.6189	10.2247	9.8848
			MSGT	28.0963	22.2130	21.2142	20.3680	22.9601	18.7283	17.9808	17.3238
		Thai et. al. (FBT) [54]	MCST	15.8337	12.5289	11.9664	11.4769	12.7753	10.3895	9.9653	9.5967
5	1-1-1	Present	MCST	7.1113	4.5073	4.1082	3.8150	5.1421	4.5227	4.4460	4.3976
			MSGT	8.4831	5.8060	5.3896	5.0668	6.5178	5.6773	5.5586	5.4705
		Thai et. al. (FBT) [54]	MCST	7.1017	4.5053	4.1057	3.8109	5.1423	4.5238	4.4428	4.3878
	1-2-1	Present	MCST	7.1113	4.9808	4.6426	4.3784	5.5311	4.5237	4.4037	4.3362
			MSGT	8.4831	6.3453	6.0111	5.7457	6.9292	5.6181	5.4330	5.3011
		Thai et. al. (FBT) [54]	MCST	7.1017	4.9786	4.6407	4.3769	5.5301	4.5266	4.4022	4.3265
	2-1-1	Present	MCST	7.1113	4.3817	3.9772	3.6985	4.6109	4.3630	4.3365	4.3194
			MSGT	8.4831	5.6149	5.1701	4.8337	5.8653	5.3745	5.3065	5.2531
		Thai et. al. (FBT) [54]	MCST	7.1017	4.3793	3.9734	3.6906	4.6051	4.3567	4.3269	4.3050
	2-2-1	Present	MCST	7.1113	4.7285	4.3565	4.0794	4.8895	4.3715	4.3167	4.2829
			MSGT	8.4831	6.0481	5.6671	5.3716	6.2297	5.3669	5.2473	5.1551
		Thai et. al. (FBT) [54]	MCST	7.1017	4.7270	4.3548	4.0764	4.8888	4.3700	4.3110	4.2711

Table 13. Dimensionless critical buckling loads of Al/SiC sandwich microbeams ($L/h = 10, h/l = 1\ and\ 5$)

h/ℓ	Types	Theory		Type A				Type B			
				$p_z = 0$	1	2	5	$p_z = 0$	1	2	5
1	1-1-1	Present	MCST	365.0902	201.5335	177.8299	158.6025	245.6529	178.6914	168.3499	159.7368
			MSGT	1109.4730	618.6074	544.7599	484.9035	770.3131	565.8243	533.1584	505.3672
		Thai et. al. (FBT) [54]	MCST	352.1681	198.0034	174.9327	155.7847	238.4427	170.7500	159.4940	149.8573
	1-2-1	Present	MCST	365.0902	237.4562	218.5547	203.0833	272.3210	170.0736	154.4970	141.6387
			MSGT	1109.4730	729.7802	671.1393	622.7724	846.7941	536.0448	486.4989	444.3438
		Thai et. al. (FBT) [54]	MCST	352.1681	232.7431	214.6634	199.7249	264.7995	162.6654	146.2180	132.4253
	2-1-1	Present	MCST	365.0902	185.4124	159.5378	138.6359	196.9300	149.7151	142.3269	136.0824
			MSGT	1109.4730	571.6292	492.4064	428.2822	625.1140	471.4704	446.7637	425.6525
		Thai et. al. (FBT) [54]	MCST	352.1681	181.5212	155.9268	134.6181	187.5531	140.6339	132.8920	126.2934
	2-2-1	Present	MCST	365.0902	216.3865	194.6101	176.9155	225.5102	148.2970	136.3331	126.2689
			MSGT	1109.4730	667.0363	600.4412	546.1704	711.4946	465.7922	426.0570	392.0621
		Thai et. al. (FBT) [54]	MCST	352.1681	212.0386	190.8467	173.1709	217.8015	140.2876	127.8655	117.4541
5	1-1-1	Present	MCST	71.0972	27.3357	22.3708	18.9991	35.7426	27.1789	26.0926	25.3525
			MSGT	101.1644	45.3529	38.4965	33.5091	57.4192	42.8253	40.7840	39.2317
		Thai et. al. (FBT) [54]	MCST	70.9041	27.3105	22.3426	18.9578	35.6265	26.9987	25.8502	25.0248
	1-2-1	Present	MCST	71.0972	33.7540	29.0008	25.5052	41.7385	27.1845	25.5056	24.4668
			MSGT	101.1644	54.7745	48.6112	43.9151	65.4972	41.9278	38.8210	36.5707
		Thai et. al. (FBT) [54]	MCST	70.9041	33.7239	28.9761	25.4867	41.6396	27.0317	25.2836	24.1451
	2-1-1	Present	MCST	71.0972	25.7092	20.8308	17.7096	28.2228	24.9081	24.4720	24.1413
			MSGT	101.1644	42.2116	35.1954	30.2445	45.6635	37.7966	36.6465	35.7105
		Thai et. al. (FBT) [54]	MCST	70.9041	25.6667	20.7741	17.6157	27.9689	24.6248	24.1493	23.7663
	2-2-1	Present	MCST	71.0972	30.2383	25.3304	21.9149	32.0846	25.0737	24.2366	23.6381
			MSGT	101.1644	49.4633	42.8577	37.9924	52.0779	37.7936	35.8159	34.2522
		Thai et. al. (FBT) [54]	MCST	70.9041	30.2047	25.2938	21.8645	31.9293	24.8576	23.9701	23.3079

Table 14. Dimensionless deflections of Al/SiC sandwich microbeams for various (L/h) and (h/ℓ)

L/h	h/ℓ	Type A (1-1-1)				Type B (1-1-1)			
		$p_z = 0$	1	2	5	$p_z = 0$	1	2	5
S-S									
5	1	18.7134	16.2372	15.2689	14.2027	16.0169	14.3904	13.8048	13.2039
	2	14.3529	11.6723	10.7556	9.8562	11.7581	10.6205	10.2269	9.8316
	4	8.9867	7.1059	6.4733	5.8743	7.0681	6.3812	6.1553	5.9437
	8	7.0075	5.2546	4.6589	4.1215	5.1585	4.6652	4.5109	4.3802
20	1	28.5660	24.2197	22.6310	20.9499	24.4148	22.0491	21.2309	20.3872
	2	15.3703	12.7769	11.8623	10.9296	12.8314	11.5975	11.1784	10.7576
	4	9.5514	7.5436	6.8638	6.2192	7.5180	6.8176	6.5904	6.3793
	8	7.4120	5.4933	4.8515	4.2776	5.4219	4.9432	4.7986	4.6825
C-F									
5	1	9.8635	8.2039	7.5986	6.9798	8.3707	7.6162	7.3526	7.0787
	2	5.3179	4.3796	4.0531	3.7259	4.4287	4.0196	3.8805	3.7403
	4	3.3141	2.6189	2.3842	2.1618	2.6163	2.3739	2.2949	2.2212
	8	2.5761	1.9192	1.6979	1.4993	1.8956	1.7261	1.6742	1.6315
20	1	10.2072	8.6734	8.1135	7.5188	8.7358	7.8857	7.5921	7.2894
	2	5.4906	4.5687	4.2432	3.9106	4.5871	4.1457	3.9957	3.8452
	4	3.4107	2.6936	2.4507	2.2204	2.6850	2.4357	2.3548	2.2797
	8	2.6461	1.9602	1.7309	1.5260	1.9355	1.7654	1.7142	1.6731
C-C									
5	1	43.9499	38.0208	35.7394	32.3018	36.5150	32.1641	30.7289	29.3699
	2	28.4376	22.2283	20.2552	18.4441	23.4401	21.8576	21.3255	20.7856
	4	17.8605	14.1171	12.8912	11.7441	14.4205	13.1904	12.7805	12.3835
	8	13.9255	10.7518	9.6390	8.6146	10.7353	9.7280	9.3944	9.0821
20	1	63.6928	53.2683	49.4555	45.5144	54.2003	49.2517	47.5298	45.7423
	2	34.3239	28.3474	26.2586	24.1540	28.6202	25.9621	25.0587	24.1496
	4	21.3760	16.8864	15.3696	13.9321	16.8670	15.3118	14.8066	14.3358
	8	16.6086	12.3488	10.9180	9.6354	12.2026	11.1239	10.7959	10.5284

Table 15. Dimensionless critical buckling loads of Al/SiC sandwich microbeams for various (L/h) and (h/ℓ)

L/h	h/ℓ	Type A (1-1-1)				Type B (1-1-1)			
		$p_z = 0$	1	2	5	$p_z = 0$	1	2	5
S-S									
5	1	164.9208	103.2696	85.2182	69.3736	111.5575	92.7174	86.6215	80.4804
	2	48.2818	30.4919	25.4914	21.0771	31.8818	26.1026	24.2967	22.5505
	4	18.9526	11.3385	9.2704	7.5205	11.4332	9.2521	8.5971	8.0033
	8	11.5344	6.2116	4.8118	3.7103	6.0950	4.9427	4.6113	4.3361
20	1	186.9813	128.6458	110.6457	93.3825	130.9024	104.4936	96.1890	88.0542
	2	54.1339	35.8031	30.4002	25.4170	36.1526	28.9028	26.6578	24.5088
	4	20.9045	12.4807	10.1785	8.2299	12.4105	9.9876	9.2654	8.6182
	8	12.5886	6.6184	5.0853	3.8935	6.4551	5.2506	4.9122	4.6431
C-F									
5	1	45.4382	30.5524	25.9895	21.6977	31.5697	25.4588	23.5142	21.5883
	2	13.1983	8.6352	7.3039	6.0897	8.7913	7.0691	6.5321	6.0193
	4	5.1175	3.0570	2.4945	2.0184	3.0493	2.4570	2.2801	2.1212
	8	3.0898	1.6329	1.2568	0.9637	1.5947	1.2963	1.2120	1.1444
20	1	47.0672	32.5831	28.1096	23.7928	33.0236	26.2930	24.1813	22.1164
	2	13.6165	9.0310	7.6758	6.4225	9.1001	7.2649	6.6969	6.1536
	4	5.2527	3.1357	2.5570	2.0671	3.1158	2.5067	2.3252	2.1627
	8	3.1612	1.6599	1.2748	0.9757	1.6184	1.3167	1.2320	1.1648
C-C									
5	1	507.9896	282.0742	224.1624	178.2289	329.0644	288.7739	275.7977	262.5040
	2	149.8475	87.8151	71.8537	58.6611	97.5278	83.0408	78.5206	74.1035
	4	59.6361	35.7448	29.3702	23.9998	37.2474	30.5117	28.4489	26.5261
	8	36.6710	20.8600	16.4863	12.9441	20.7997	16.7480	15.5217	14.4177
20	1	728.3100	489.7552	416.6431	348.0825	505.7471	407.6671	376.5705	345.9169
	2	211.4368	138.3596	117.0409	97.5834	140.8304	113.2060	104.6317	96.4027
	4	81.9669	48.9569	39.9471	32.3214	48.8242	39.3393	36.5079	33.9646
	8	49.4744	26.1421	20.1203	15.4274	25.5274	20.7509	19.4023	18.3194

Table 16. Dimensionless fundamental frequency of Al/SiC sandwich microbeams for various (L/h) and (h/ℓ)

L/h	h/ℓ	Type A (1-1-1)				Type B (1-1-1)			
		$p_z = 0$	1	2	5	$p_z = 0$	1	2	5
S-S									
5	1	1.5294	2.4395	2.9554	3.6299	2.2602	2.7204	2.9125	3.1350
	2	5.2241	8.2655	9.8848	11.9535	7.9097	9.6643	10.3837	11.1894
	4	13.3081	22.2449	27.2090	33.5427	22.0679	27.2733	29.3521	31.5301
	8	21.8675	40.6300	52.4607	68.0480	41.4140	51.0650	54.7312	58.1978
20	1	1.3517	1.9643	2.2836	2.7055	1.9306	2.4188	2.6277	2.8706
	2	4.6690	7.0588	8.3131	9.9426	6.9911	8.7451	9.4818	10.3134
	4	12.0912	20.2523	24.8330	30.7131	20.3673	25.3085	27.2814	29.3302
	8	20.0790	38.1933	49.7084	64.9246	39.1600	48.1427	51.4588	54.4410
C-F									
5	1	5.0248	7.7923	9.3160	11.3007	7.3399	8.9456	9.6209	10.4031
	2	17.2492	26.9597	32.1008	38.6826	26.0095	31.9933	34.4667	37.2431
	4	44.2740	74.0792	90.6657	111.8429	73.6550	91.1373	98.1235	105.4305
	8	73.1597	136.5927	176.6321	229.3987	139.3220	171.6702	183.8897	195.3314
20	1	4.5892	6.6593	7.7361	9.1585	6.5512	8.2125	8.9237	9.7504
	2	15.8548	23.9557	28.2061	33.7292	23.7359	29.7004	32.2060	35.0349
	4	41.0705	68.7936	84.3557	104.3331	69.1929	85.9845	92.6890	99.6510
	8	68.2149	129.7859	168.9281	220.6527	133.0769	163.5973	174.8614	184.9856
C-C									
5	1	0.4028	0.7263	0.9136	1.1481	0.6217	0.7084	0.7417	0.7793
	2	1.3683	2.3400	2.8605	3.5028	2.1019	2.4672	2.6089	2.7641
	4	3.4578	5.7759	7.0283	8.5952	5.5237	6.7382	7.2261	7.7507
	8	5.6761	9.9381	12.5469	15.9427	9.9342	12.3421	13.3243	14.3594
20	1	0.2790	0.4163	0.4900	0.5871	0.4022	0.4983	0.5392	0.5867
	2	0.9608	1.4710	1.7399	2.0876	1.4431	1.7937	1.9400	2.1049
	4	2.4779	4.1485	5.0837	6.2821	4.1570	5.1580	5.5577	5.9737
	8	4.1051	7.7602	10.0788	13.1400	7.9445	9.7745	10.4553	11.0760

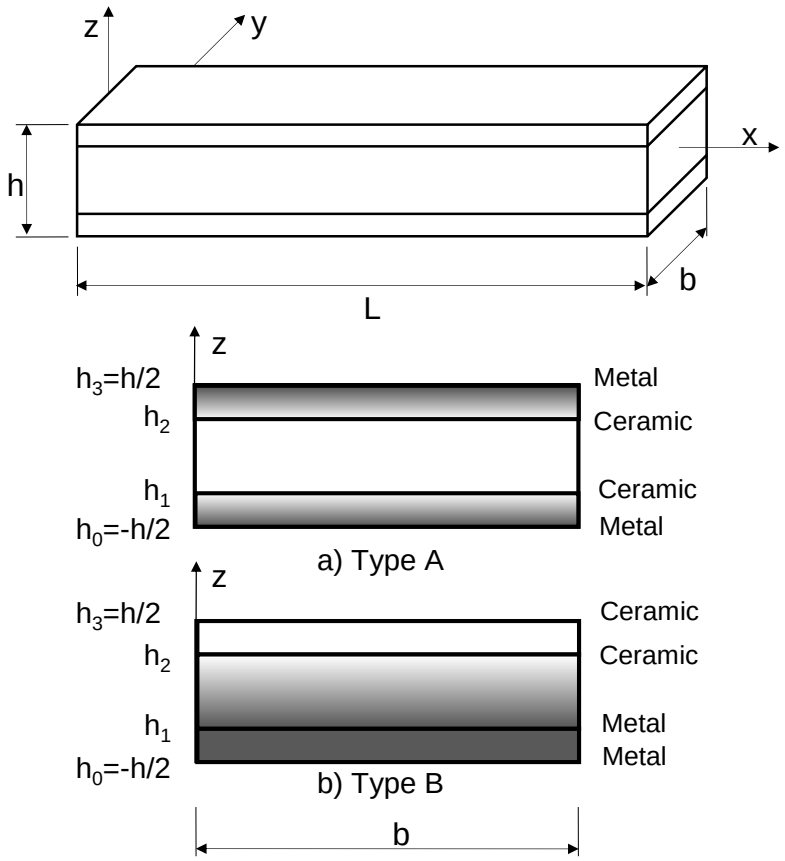

Figure 1. Geometry and coordinate of a FG sandwich beam

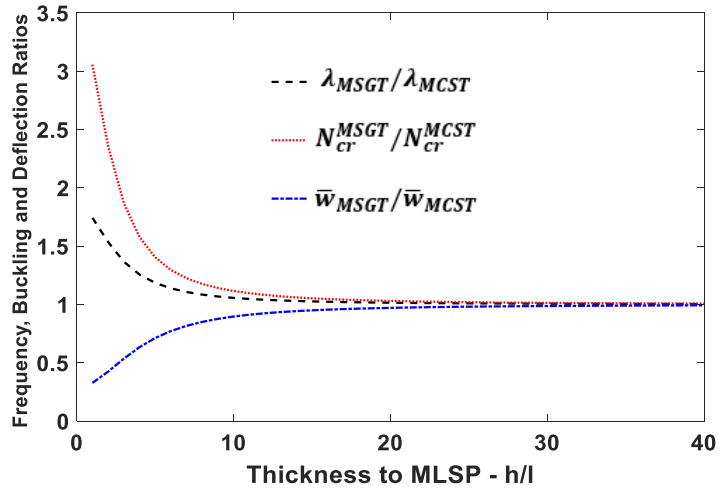

a) S-S

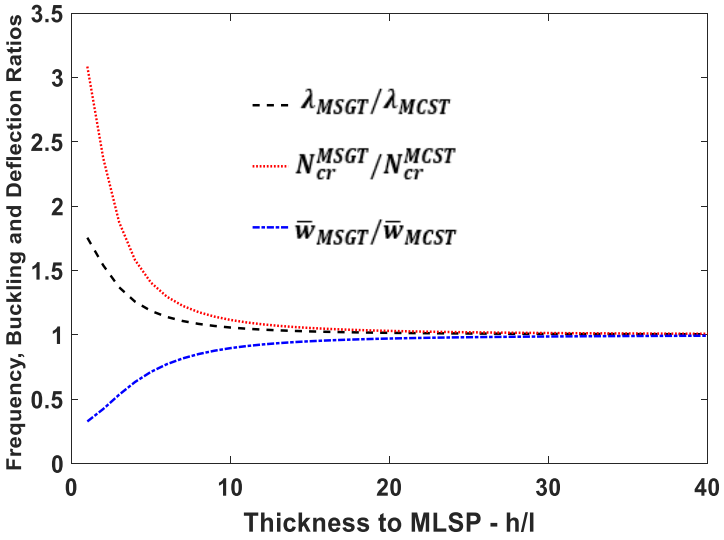

b) C-F

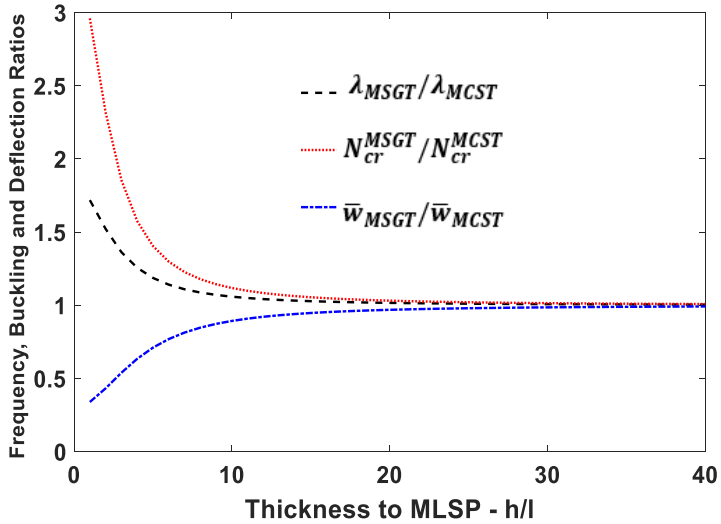

c) C-C

Figure 2. Comparison of the size effect of the MCST and MSGT on the frequency, buckling and deflection ratios for Al/SiC microbeams with respect to various BCs and (h/l) $(\ell_0 = \ell_1 = \ell_2 = \ell = 15\mu m, L/h = 10, p_z = 5$

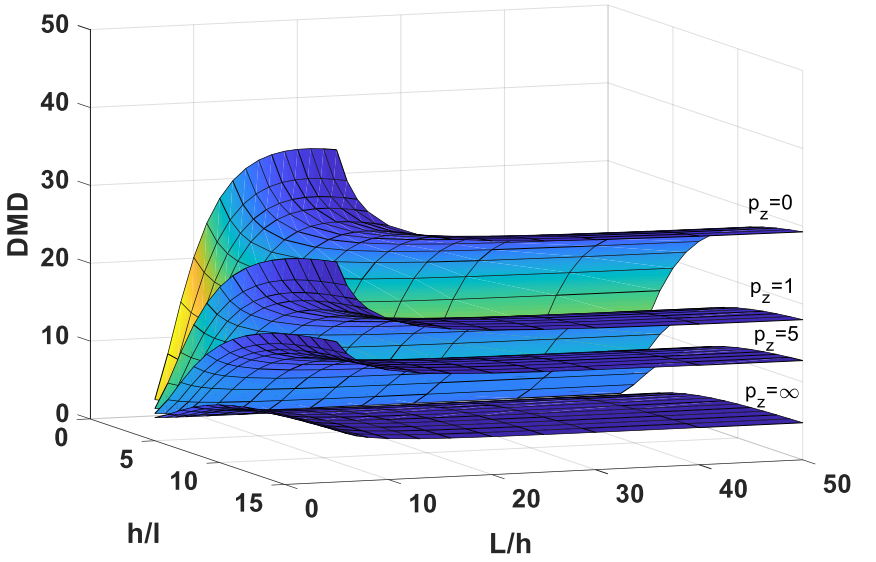

a) DMD

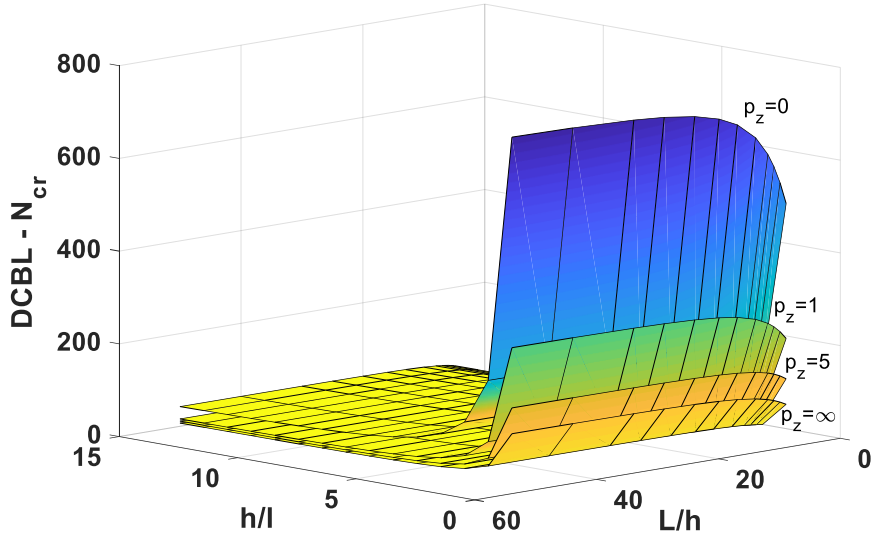

b) DCBL

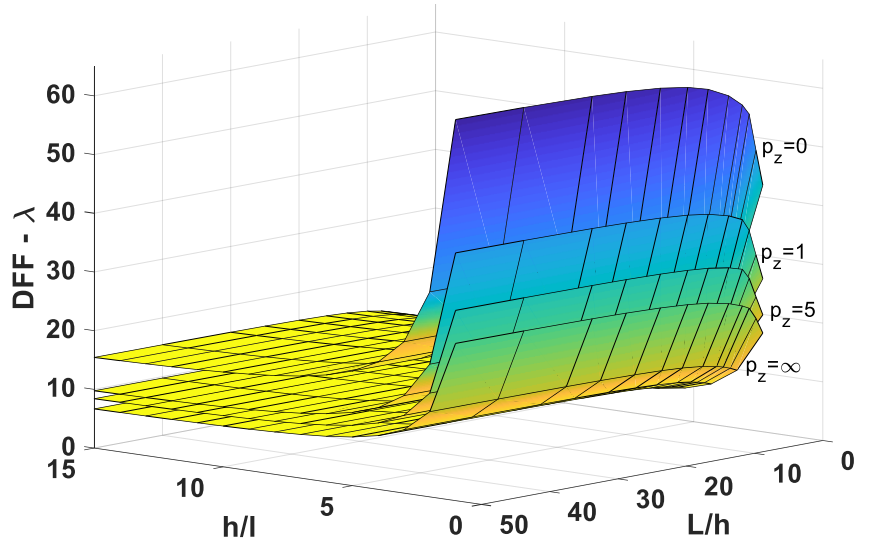

c) DFF

Figure 3. DMD/DBCL/DFF of Al/SiC C-C microbeams ($\ell_0 = \ell_1 = \ell_2 = \ell = 15\mu m, L/h, h/l, p_z = 0, 1, 5, \infty$).

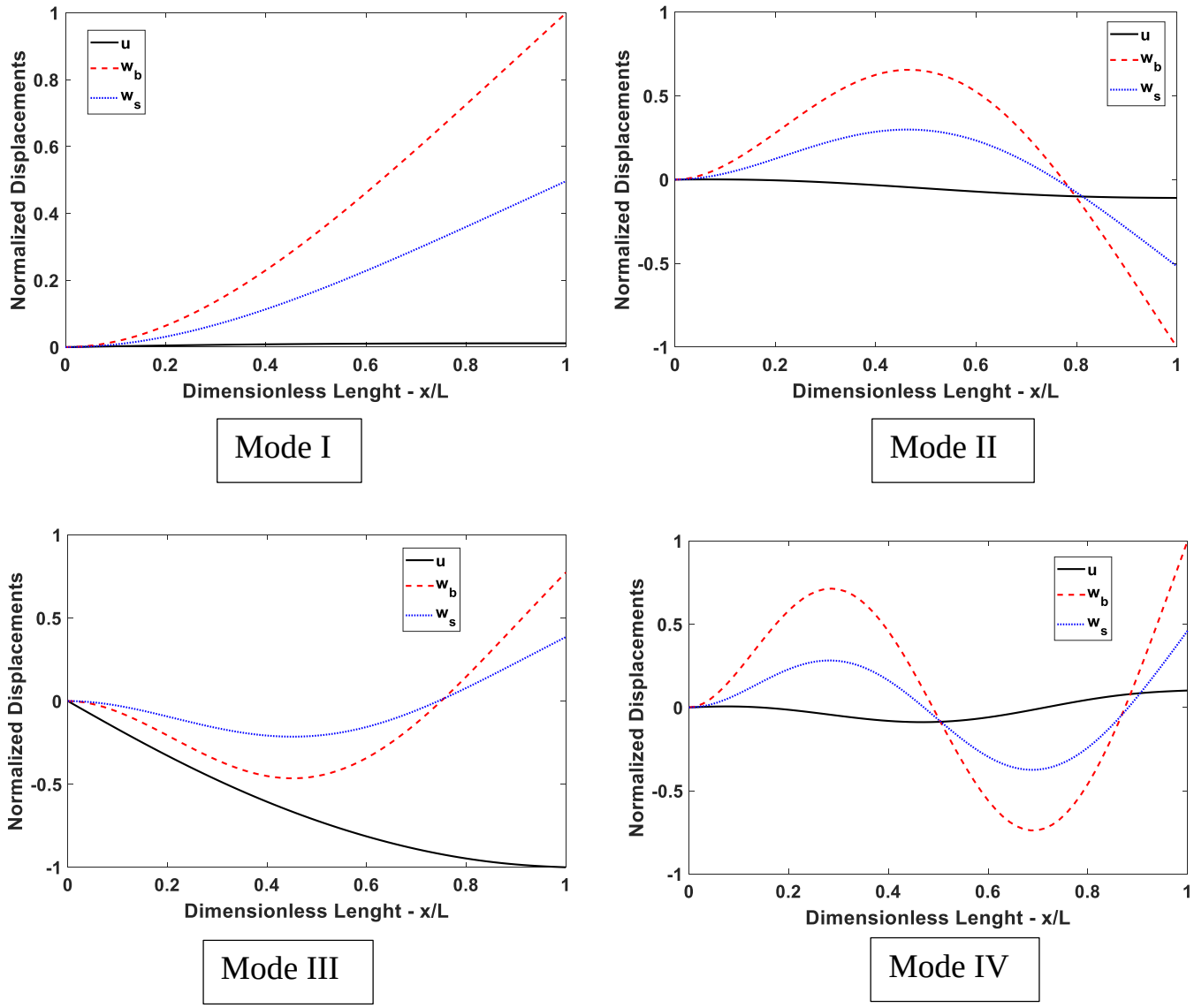

Figure 4. The first four vibration mode shapes of Al/SiC C-F microbeams ($\ell_0 = \ell_1 = \ell_2 = \ell = 15\mu m, L/h = 10, p_z = 5$).

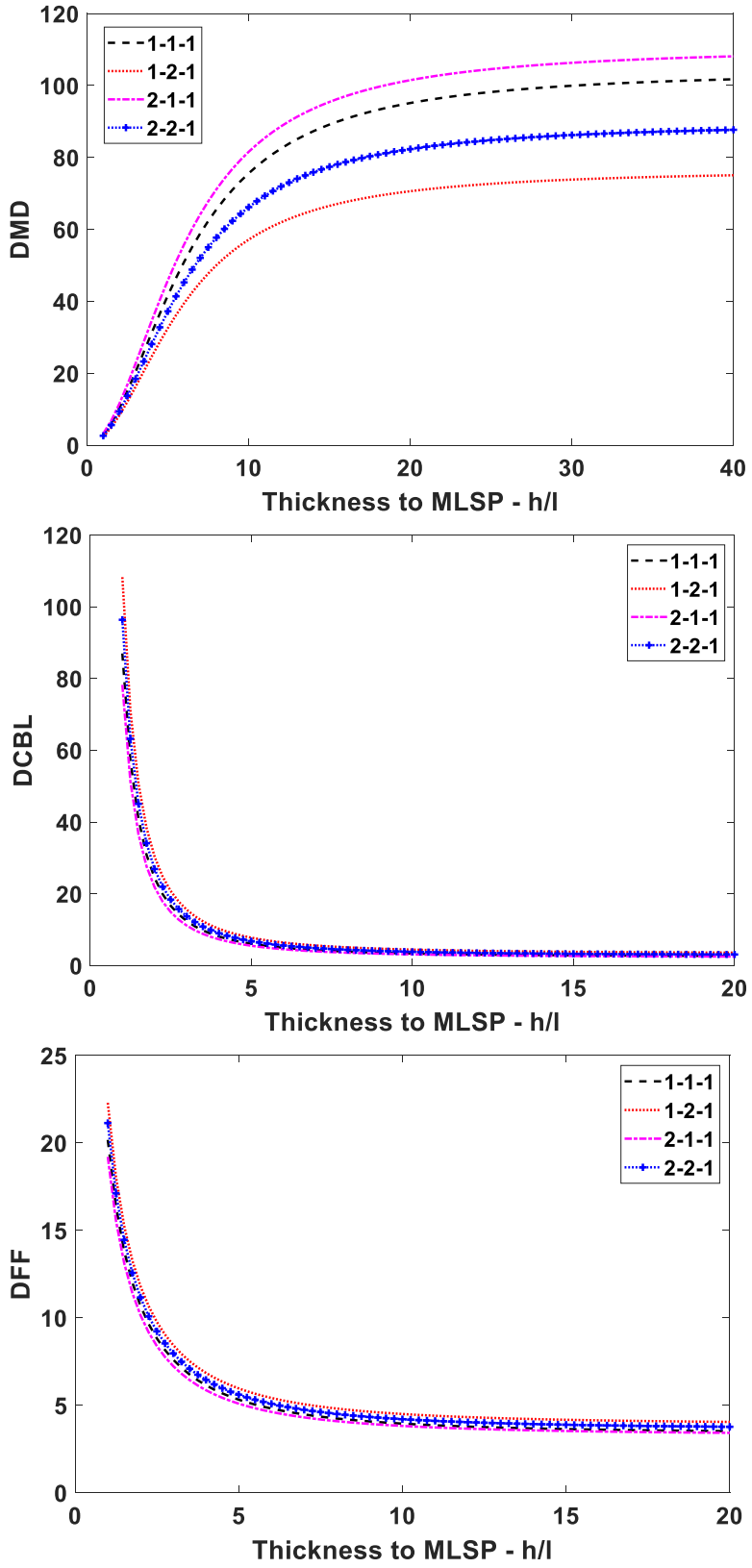

a) DMD

b) DCBL

c) DFF

Figure 5. DMD/DCBL/DFF of Al/SiC sandwich S-S microbeams (Type A) for various (h/l) $(\ell_0 = \ell_1 = \ell_2 = \ell = 15\mu m, L/h = 10, p_z = 5)$.

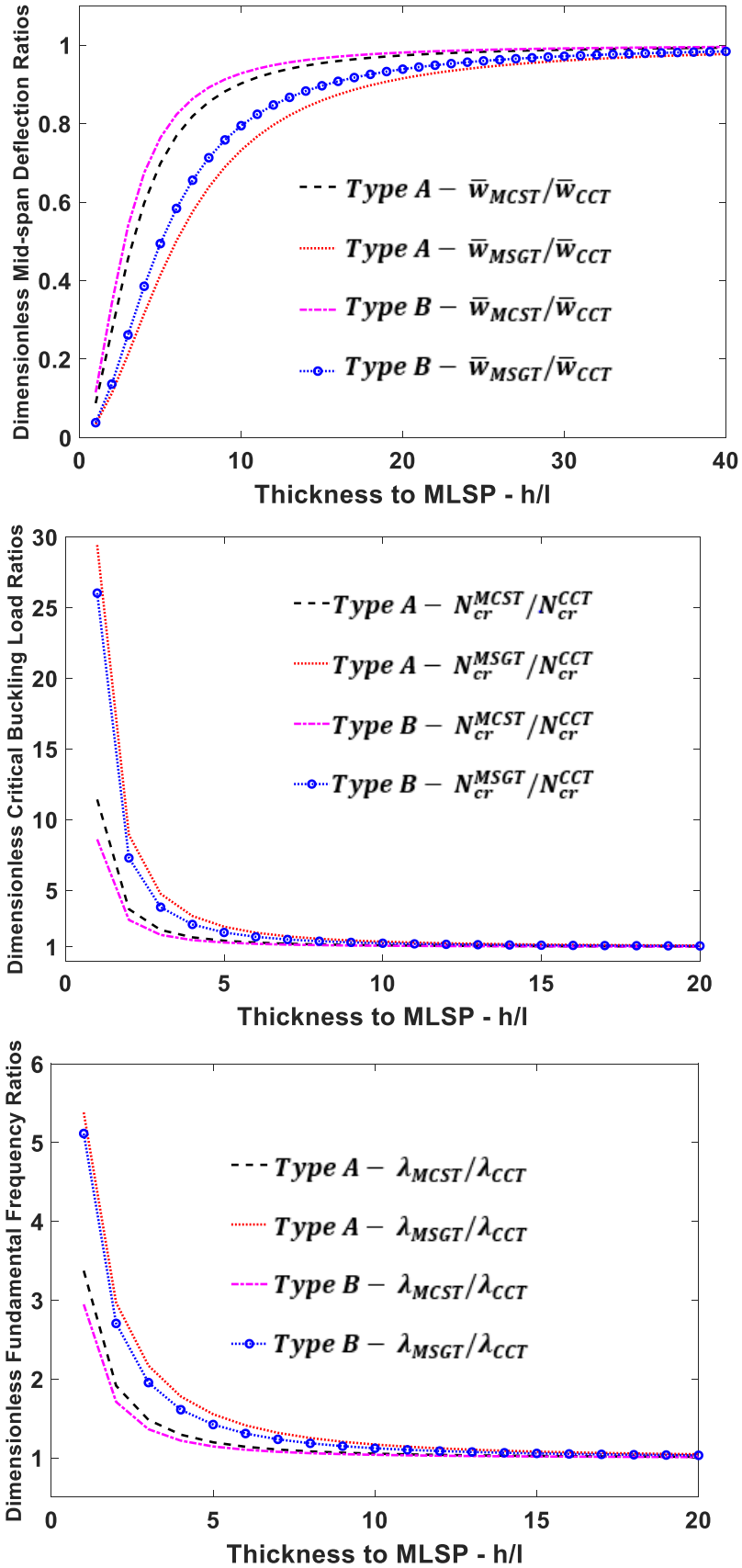

Figure 6. Comparison of the size effect of the MCST and CCT on the frequency, buckling and deflection ratios for Al/SiC sandwich C-C microbeams (1-1-1, Type A and B) for various (h/l) $(\ell_0 = \ell_1 = \ell_2 = \ell = 15\mu m, L/h = 10, p_z = 5)$.

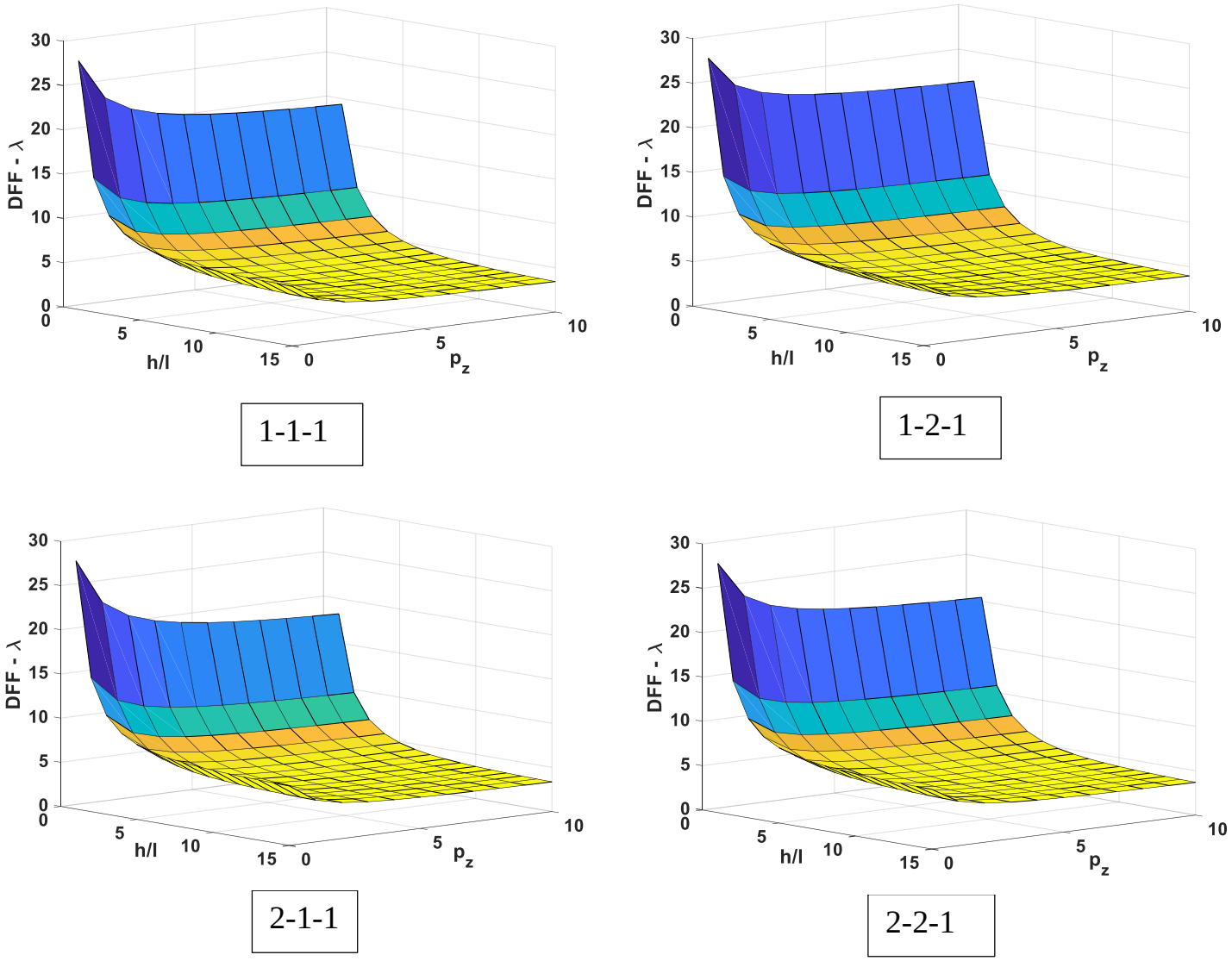

Figure 7. DFFs of Al/SiC sandwich S-S microbeams (Type A) for various p_z and (h/l) ($\ell_0 = \ell_1 = \ell_2 = \ell = 15\mu m, L/h = 10$).